Gamma radiolysis of TODGA and CyMe$_4$BTPhen in the ionic liquid tri-*n*-octylmethylammonium nitrate

Peter Zsabka[a,b], Karen Van Hecke[a], Andreas Wilden[c], Giuseppe Modolo[c], Michelle Hupert[d], Vincent Jespers[e], Stefan Voorspoels[e], Marc Verwerft[a], Koen Binnemans[b], Thomas Cardinaels[a,b,*]

[a]*Belgian Nuclear Research Center (SCK·CEN), Institute for Nuclear Materials Science, Boeretang 200, B-2400 Mol, Belgium,*

[b] *KU Leuven, Department of Chemistry, Celestijnenlaan 200F, P.O. Box 2404, B-3001 Heverlee, Belgium*

[c] *Forschungszentrum Jülich GmbH, Institut für Energie- und Klimaforschung – Nukleare Entsorgung und Reaktorsicherheit (IEK-6), 52428 Jülich, Germany*

[d] *Forschungszentrum Jülich GmbH, Zentralinstitut für Engineering, Elektronik und Analytik (ZEA-3), 52428 Jülich, Germany*

[e] *Flemish Institute for Technological Research (VITO NV)), Boeretang 200, B-2400 Mol, Belgium,*

*Corresponding author. Email: tcardina@sckcen.be

Abstract

Radiolytic stability of the extractants *N,N,N',N'*-tetraoctyl diglycolamide (TODGA) and 2,9-bis(5,5,8,8-tetramethyl-5,6,7,8-tetrahydro-1,2,4-benzotriazin-3-yl)-1,10-phenanthroline (CyMe$_4$BTPhen) in the ionic liquid tri-*n*-octylmethylammonium nitrate ([N$_{1888}$][NO$_3$]) was studied via the combination of a steady-state irradiation by cobalt-60 gamma-radiation, followed by solvent extraction and identification of radiolysis products by High Performance Liquid Chromatography coupled to Electro Spray Ionisation (HPLC-ESI-MS). The observed trend for the distribution ratios of trivalent minor actinides and Eu(III) showed a decrease as a function of absorbed dose in the case of the TODGA solvent. The gamma irradiations were conducted in the presence or absence of an acidic aqueous phase. The determined dose constants for TODGA under neutral or acidic conditions were up to four times lower than the values reported in aliphatic diluents under comparable conditions. The degradation patterns were similar to those found by former studies on TODGA diluted in *n*-dodecane; only de-alkylation and bond ruptures within the diglycolamide core were observed. The presence of an acidic aqueous phase during irradiation resulted in a different relative abundance of certain radiolysis products of both the diluent and TODGA and a higher dose constant compared to the neutral irradiation conditions. A quantification of CyMe$_4$BTPhen in irradiated samples with the [N$_{1888}$][NO$_3$] diluent was not possible, but the effect on its extraction properties was evaluated. The distribution ratios slightly increased under the effect of absorbed dose, indicating the formation of a radiolysis product(s) that are efficient extractants as well.

Keywords: solvent extraction; TODGA; CyMe$_4$BTPhen, gamma radiolysis; ionic liquids; HPLC-ESI-MS

1. Introduction

Chemical research in the context of the Partitioning and Transmutation strategy (P&T) of reprocessing of spent nuclear fuel aims at the separation of minor actinides (MA, i.e. americium, curium and neptunium) from the highly active raffinate originating from the spent fuel reprocessing.[1, 2] Neptunium separation is feasible in an advanced PUREX (plutonium uranium reduction extraction) flow sheet, while americium and curium are currently rejected to the highly active waste. However, an efficient removal of americium and curium from the highly active waste could not only contribute to a significant decrease of the long-term radiotoxicity and heat load of the vitrified highly active waste, but also to the development of a more sustainable nuclear fuel cycle.[3, 4] The main challenges in implementing minor actinide separation processes are the presence of high concentrations of HNO_3 and chemically similar lanthanides, as well as the high radiation dose rate which causes solvent degradation.

European large-scale research projects (e.g. the latest SACCESS[5, 6] and GENIORS[7] projects) elaborated hydrometallurgical partitioning processes for spent light water reactor fuel, as well as pyrometallurgical processes relevant for the treatment of spent fuel envisaged for GenIV reactors.[8] In order to minimize the secondary waste stemming from hydrometallurgical processes (e.g. via complete incineration), the applied chemicals should preferably consist of only four elements: carbon (C), hydrogen (H), oxygen (O) and nitrogen (N) (CHON principle).[9] Partitioning process development was mainly aiming for a strategy where all the requirements could be met by a single system.[10] For the An(III)+Ln(III) co-extraction step in the diamide extraction (DIAMEX)[11] originally the malonamide DMDOHEMA and more recently the glycolamide *N,N,N',N'*-tetraoctyl diglycolamide (TODGA), (both solvating extractants)[12, 13] were selected as reference molecules in combination with the aliphatic molecular diluent *n*-dodecane. Previous investigations on the effect of the gamma irradiation of organic solvents composed of TODGA or other diglycolamides (DGAs) in *n*-dodecane or 1-octanol revealed that the molecules of these diluents form radical cations in high yield due to their low ionization potential.[14] The dose constant of TODGA was found to depend on its molar concentration in the aliphatic diluent. In fact the concentration of radical cations formed from diluent radiolysis influences the ligand degradation rate via charge transfer reactions between radical cations and the ligand (this radiolysis pathway is called the “sensitization effect”). Speciation studies identified that the main degradation products can be derived from the break of bonds within the DGA part of the molecule and via de-alkylations.[15-18]

Selective minor actinide extraction processes were developed making use of the highly selective soft-donor ligands 6,6’-bis(5,5,8,8- tetramethyl-5,6,7,8- tetrahydro-1,2,4-benzotriazine-3-yl)-2,2’-bipyridine ($CyMe_4BTBP$)[19, 20] and the *cis*-locked extractant 2,9-bis(5,5,8,8- tetramethyl-5,6,7,8- tetrahydro-1,2,4- benzotriazine-3-yl)-1,10-phenanthroline ($CyMe_4BTPhen$) (Figure 1).[21, 22] In these processes, the trivalent minor actinides are separated from trivalent lanthanides. Previous radiation stability studies of solvents composed of 1-octanol and $CyMe_4BTBP$ [23, 24] or $CyMe_4BTPhen$ [25] revealed that the ligands undergo addition reactions with α-hydroxyoctyl radicals formed from diluent radiolysis. This type of adduct formation was previously discovered in irradiated solutions of (2,6-bis(5-(2,2-dimethylpropyl)-1*H*-pyrazol-3-yl)pyridine (C5-BPP) in 1-octanol.[26] One approach to improve radiation stability of the system could be the complete or at least partial replacement of 1-octanol by a co-diluent, which is more resistant to radiation-induced degradation. Such diluent mixtures of 1-octanol/toluene and 1-octanol/ hydrogenated tetrapropylene (TPH) were tested by Lewis *et al.*[21] A radiolysis study using $CyMe_4BTBP$ and $CyMe_4BTPhen$ in phenyl trifluoromethyl sulfone (FS-13), confirmed that both extraction properties and the resistance against radiolytic degradation can be improved if the 1-octanol diluent is replaced.[27]

Ionic liquids have been proposed as a replacement of aliphatic molecular organic diluents for MA partitioning.[28-31] Tri-*n*-octyl-methylammonium nitrate ($[N_{1888}][NO_3]$), a CHON-complying, hydrophobic room-temperature ionic liquid, was used recently as a diluent in minor actinide partitioning studies.[32-34] Water-saturated $[N_{1888}][NO_3]$ ionic liquid and its mixtures with extractants are not isotropic solutions, they form aggregates the size of which is a function of nitric acid or metal loading or ligand concentration.[35] Due to its polar nature the ionic liquid is capable of stabilizing these aggregate or supramolecular structures to such an extent that third phase (or splitting of the organic phase) does not occur.

All solvents (composed of an extractant and a diluent) used in nuclear fuel cycle processes are exposed to α, β and γ radiation. Both the diluent and solute molecules can undergo ionization, excitation or form radicals upon reacting with the secondary electrons formed from the incident photons and charged particles or upon reacting with any of the radiolysis products. However, the probability of interaction of molecules in a solution with the incident photons or charged particles occur in proportion to their relative abundance, thus direct radiolysis plays usually a minor role in the degradation of solutes present in low concentrations.[36, 37] The reactive radical species are responsible for the chemical reactions that occur with the solutes present in the solvent at low concentration, a reaction that is referred to as indirect radiolysis. In the case of biphasic systems or water-equilibrated organic phases, the radiolysis of water is of prime importance for the fate of solutes. The pH and dissolved oxygen content of the irradiated aqueous solution has a large effect on the speciation of the primary radiolysis products of water.[38] At high acidity and under aerated conditions, the main species present are $^{\bullet}OH$ radical and atomic hydrogen, while solvated electrons are rapidly scavenged by the protons. Above pH ~ 4, the solvated electron becomes equally abundant species as the $^{\bullet}OH$ radical. Irradiated neutral aqueous solutions under aerated condition yield oxidizing $^{\bullet}OH$ radicals, solvated electrons, hydrogen atoms and hydrogen peroxide. In the presence of nitric acid, $^{\bullet}NO_2$ and $^{\bullet}NO_3$ radicals are formed, as well as nitrous ions or nitrous acid.[38, 39] Radiolysis of organic solutions composed of an alkane diluent yields neutral and cationic carbon-centered radicals.[36]

The available information on the radiolytic stability of ionic liquids is limited compared to radiolysis of aqueous solutions or aliphatic solvents and only a few classes of ionic liquids were subject to radiolysis studies. A comprehensive review on the existing literature on radiolytic stability of ionic liquids was compiled by Mincher and Wishart.[40] Due to the radiolytic formation of HF and other volatile fluorinated species, the most common, fluorinated ionic liquids are considered unsuitable in nuclear fuel cycle applications.[41, 42] Therefore, the fluorine-free ionic liquid tri-*n*-octylmethylammonium nitrate $[N_{1888}][NO_3]$ was investigated in this study. Radiolysis studies on $[N_{1888}][NO_3]$ have not been described in open literature before. In the case of a short chain length quaternary ammonium ionic liquid, $[N_{1444}][Tf_2N]$ where the hydrophobicity is provided by a fluorinated anion, gamma radiation (^{137}Cs up to 2 MGy absorbed dose) caused N-C_{butyl} or N-C_{methyl} bond break, H-abstraction or double bond formation.[43] It was found that covalently bound adducts were formed between the primary radiolysis products of the anions ($CF_3^{\bullet -}$, $NSO_2^{\bullet -}$ and $NSO_2CF_3^{\bullet -}$) and the $[N_{1444}]^+$ cation. γ (^{60}Co) and ion-beam (H^+ or $^4He^{2+}$) radiolysis of a series of quaternary ammonium bistriflimide ionic liquids ($[N_{1114}][Tf_2N]$, $[N_{2226}][Tf_2N]$, $[N_{2228}][Tf_2N]$ and $[N_{112(12)}][Tf_2N]$) caused H_2 production.[44] The production of H_2 increased with the increase of aliphatic chain length of the cation, however, the correspondence was not linear.

The γ radiation stability of [A336][Cl] was studied by Jagadeeswara Rao *et al.*[45] [A336][Cl] (or Aliquat 336) is a commercially available mixture of quaternary ammonium chlorides with tri-*n*-octylmethylammonium chloride as main component. Changes in density, viscosity and refractive indices were found to be insignificant for the investigated 400 and 700 kGy absorbed doses. The electrochemical window of the nitrate ionic liquid [A336][NO_3] decreased from 4.319 V to 3.464 V upon the absorption of 700 kGy γ – dose. [N_{1888}][NO_3] is the main component of the ionic liquid [A336][NO_3].[46-48] For fundamental studies, especially when NMR or mass spectra have to be recorded, the use of [N_{1888}][NO_3] is preferred over the mixture [A336][NO_3]. The radiation stability of a system composed of 0.1 mol L^{-1} bis(2-ethylhexyl)diglycolamide (T2EHDGA) in [N_{1888}][NO_3] was studied via solvent extraction by Venkateswara Rao *et al.*[35] The distribution ratios of Eu(III) and Am(III) were unchanged up to 500 kGy absorbed γ dose. From this observation it was hypothesized that the ionic liquid undergoes sacrificial degradation, resulting in a low indirect radiolysis of the extractants.

In the present paper, the effect of γ radiation from a pool-type ^{60}Co source on two ionic liquid based solvents was investigated. Batch solvent extraction studies were conducted on the irradiated solvents together with analysis of the radiolysis products using a Ultra High-Performance Liquid Chromatography (UHPLC) coupled to an electrospray-ionization (ESI) mass spectrometry (MS) method. Irradiations were conducted on samples of 0.05 mol L^{-1} TODGA in [N_{1888}][NO_3] both in the presence and absence of 2.5 mol L^{-1} HNO_3 to compare the effect of nitric acid on the ligand degradation rates. A second solvent containing 0.01 mol L^{-1} of the soft-donor extractant $CyMe_4BTPhen$ in [N_{1888}][NO_3] was irradiated in the presence or absence of 1 mol L^{-1} HNO_3.

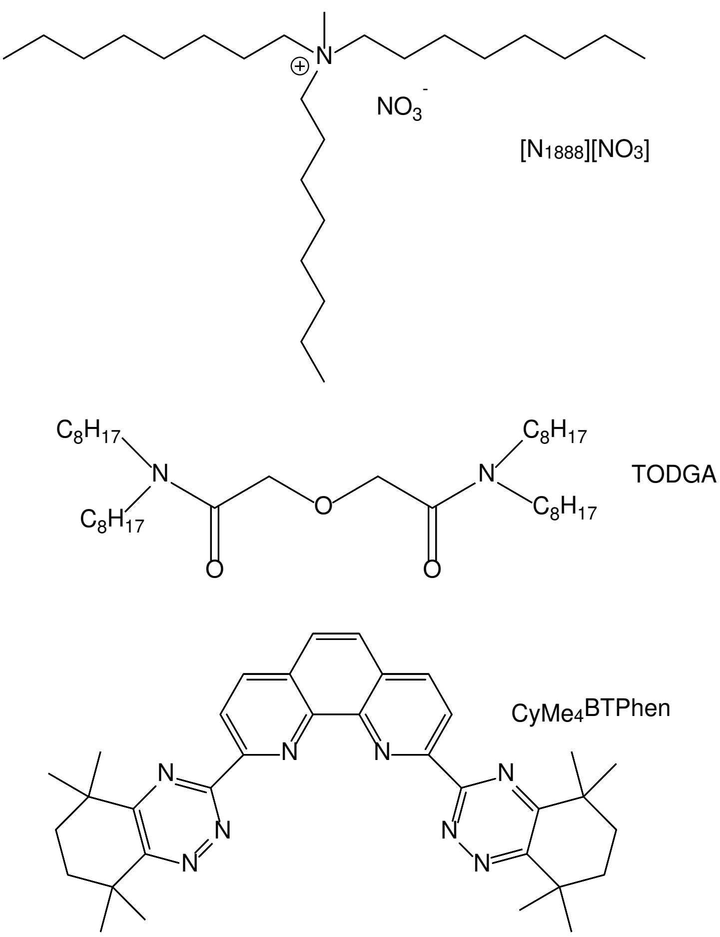

Figure 1. Chemical structures with the acronyms of the compounds used in this study.

2. Experimental

2.1 Chemicals

Tri-*n*-octylmethylammonium chloride [N_{1888}][Cl] (purity: > 97.0 %) was obtained from Sigma-Aldrich (Steinheim, Germany). *N,N,N',N'* – tetraoctyl diglycolamide (TODGA, purity: 99 %) and 2,9-bis(5,5,8,8-tetramethyl-5,6,7,8-tetrahydro-1,2,4-benzotriazin-3-yl)-1,10-phenanthroline ($CyMe_4BTPhen$, purity > 98 %), were purchased from Technocomm Limited (Edinburgh, UK). Potassium nitrate (purity > 97.0 %) was obtained from Merck KGaA (Darmstadt, Germany). $La(NO_3)_3{\cdot}6H_2O$ (purity: 99.0 %) was obtained from Fluka Chemie (Buchs, Switzerland); $Ce(NO_3)_3{\cdot}6H_2O$ (purity: 99.8 %), $Pr(NO_3)_3{\cdot}6H_2O$ (purity: 99.9 %), $Nd(NO_3)_3{\cdot}6H_2O$ (purity: 99.9 %), and $Sm(NO_3)_3{\cdot}6H_2O$ (purity: 99.9 %) were obtained from

Strem Chemicals (Kehl, Germany). $Eu(NO_3)_3{\cdot}6H_2O$ (purity: 99.99 %) and $Gd(NO_3)_3{\cdot}6H_2O$ (purity: 99.9 %) were obtained from Alfa Aesar (Karlsruhe, Germany). ^{241}Am tracer (radionuclidic purity > 99 %) in 1 mol L^{-1} HNO_3 solution was available from legacy stocks at SCK•CEN. ^{244}Cm (radionuclidic purity > 99.902 %) and ^{152}Eu (radionuclidic purity > 99 %) radiotracers in 1 mol L^{-1} HNO_3 solutions were obtained from Eckert and Ziegler Nuclitec GmbH (Braunschweig, Germany). MilliQ water was used for all dilutions (conductivity: > 18 MΩ cm). Technical buffer solutions were purchased from Mettler Toledo AG (Swerzenbach, Switzerland). All reagents were used as received (except $[N_{1888}][Cl]$).

The dry $[N_{1888}][Cl]$ salt was converted into the nitrate $[N_{1888}][NO_3]$ form by a metathesis reaction. The metathesis reaction was performed by stirring 100 g of $[N_{1888}][Cl]$ with 120 mL of aqueous solution of 2.5 mol L^{-1} KNO_3 for 4 hours, followed by phase separation in a 1 L separation funnel. The equilibration and separation steps were repeated seven times until no AgCl precipitation was observed any longer upon addition of drops of a $AgNO_3$ solution to the aqueous washing solution. After the metathesis reaction, the organic phase was washed three times with an equal volume of MilliQ water.

2.2. Batch solvent extraction and analytical procedures

Batch extraction studies were performed using 4 mL glass vials that fit into the boreholes of in-house fabricated metal block used as an adapter for a TMS-200 Thermoshaker (Nemus Life, Sweden). Spiked feed solutions were so prepared that 1 mL of the initial aqueous feed solution contained 3 kBq of each of the tracers ^{241}Am, ^{152}Eu and ^{244}Cm. All tracer-spiked aqueous feed solutions were prepared in advance and mixed thoroughly before adding to the known amount of organic phase.

The organic phase was either water or acid pre-equilibrated before the irradiation studies. The pre-equilibration (by water or acid) was performed once at 1:1 organic to aqueous volume ratio, at $T = (22\pm1)$ °C and 2200 rpm for 1 h. The organic phases were transferred from the original glass vials (darkened during the irradiation) to a new glass vial after irradiation, in order to be able to observe colour changes of the solvent. The organic phases that were irradiated in the presence of a 2.5 mol L^{-1} nitric acid solution were centrifuged and the clean organic phase was used for extraction studies.

A stock solution for the lanthanide-nitrate-containing aqueous phases was prepared by dissolving the calculated amounts of nitrate salts of trivalent La, Ce, Pr, Nd, Sm, Eu, Gd, Dy, Yb and Y in 0.1 mol L^{-1} HNO_3 to obtain a 10^{-3} mol L^{-1} initial concentration. From this stock solution 1 mL was taken for dilution to 100 mL in the desired final nitric acid concentration to obtain 10^{-5} mol L^{-1} final lanthanide concentration. The exact nitric acid concentration of the stock solutions was determined by titration using an autotitrator (Metrohm, Switzerland).

In a typical experiment, 500 µL of the aqueous phase was mixed with an equal volume of the organic phase and equilibrated at (22 ± 1) °C at 2200 rpm in a vial. After the equilibration, the phase disengagement was enhanced by centrifugation of the vials for 5 min at 4000 rpm using a Heraeus Labofuge 200 centrifuge. After phase separation, 300 µL aliquots of the aqueous and organic phases were collected for gamma activity measurements.

Gamma spectrometric analysis of ^{241}Am (using the 59.5 keV γ-peak) and ^{152}Eu (using the 121.8 keV, 344 keV, 778.9 keV, 964 keV, 1112 keV and 1408 keV γ-peaks) was conducted using a broad-energy range coaxial HPGe detector (model: GC2520, Canberra Semiconductors N. V., Olen, Belgium) with Genie2000 software. Samples with very low americium activity were measured also with a P-type planar germanium detector that has a higher efficiency for the low energy photons (model IGP-510, Silena Detector Systeme

GmbH, Germany). The α-particle emitter radionuclide activities were determined for each separated phase using α spectroscopy. Weighed samples of the organic or aqueous phase were pipetted on a C-1S cupped stainless steel alpha planchet (GA-MA and Associates, Inc. Florida, USA) heated under an infrared lamp (Theratherm 150 W, Osram, Germany) and subsequently burned in a gas torch. The ^{241}Am ($E_\alpha = 5.485$ MeV) and ^{244}Cm ($E_\alpha = 5.805$ MeV) α peaks were measured by an α spectrometer (Alpha Analyst, Canberra) equipped with Passivated Implanted Planar Silicon (PIPS) α detectors (Canberra Olen N.V., Olen, Belgium). The spectra were analyzed using Apex Alpha software.

The *distribution ratio* (*D*) of a given analyte was calculated as the ratio of the equilibrium concentration of the analyte present in the organic phase over the concentration present in the aqueous phase, according to equation (1).

$$D_M = \frac{[M]_{org.\ eq}}{[M]_{aq.\ eq}} \tag{1}$$

where the numerator refers to the concentration of the metal ion in the loaded ionic liquid phase, while the denominator refers to the concentration of the metal ion in the aqueous phase. The highest and lowest distribution ratio limits set by the detection limits in the aqueous or organic phases were 1000 and 0.001, respectively.

The *separation factor* (*SF*) of two elements in two phases was calculated from the distribution ratios of the respective elements in accordance with equation (2):

$$SF = \frac{D_{Mx}}{D_{My}} \tag{2}$$

The acidity of the aqueous phases was determined by either titration using an autotitrator (716 MPT Titrino, Metrohm Switzerland) filled with 0.1 mol L^{-1} or 0.01 mol L^{-1} NaOH stock solution (Titrisol, Merck) or by measurement with a pH meter (691 pH meter, Metrohm, Switzerland). The NaOH concentration was verified by titration using an oxalic acid stock solution prepared from anhydrous oxalic acid. The pH meter was calibrated prior to use with technical buffer solutions of pH = 2.00 and pH = 10.00.

2.3 Gamma-ray irradiation

The γ-ray irradiations were conducted in the Irradiations and Experiments (BEX) unit of SCK•CEN (Mol, Belgium), in a high dose-rate underwater (pool-type) ^{60}Co – source ($E_{\gamma 1}$ = 1173.24 keV and $E_{\gamma 2}$ = 1332.5 keV) at a dose-rate of 13.5 kGy h^{-1} (BRIGITTE facility). For the dose rate calibration performed at the LNK Radiation Protection Dosimetry and Calibration Laboratory in Gent[49], additionally a low dose rate pool-type facility was used (RITA) at 510 Gy h^{-1}. The ^{60}Co sources used in these pool-type irradiation facilities (RITA and BRIGITTE) are structural materials of the BR2 research reactor, that have undergone ^{59}Co(n,γ)^{60}Co activation during operation of the reactor. The high dose rate pool-type ^{60}Co gamma ray field used for the irradiation studies has a complex geometry (differences between individual ^{60}Co –sources, presence of steel structural materials and a few cm of water in between the target and the sources, air inside the irradiation chamber). Therefore, a dose rate mapping of well-defined sample positions was required. In order to define a wide range dosimetry up to the kGy h^{-1} dose rate level, alanine, ceric-cerous and Fricke dosimeters as well as polymer-based Harwell Red Perspex dosimeters (Type 4034) or Amber Perspex dosimeters (Type 3042) (Harwell Dosimetrics, Oxfordshire, UK) were used. The dose rate mapping proved that the dose rate at the used irradiation positions had a variation of less than 10 %. The samples were irradiated at a dose rate of (13.5 ± 0.9) kGy h^{-1}.

For the purpose of solvent extraction studies, one batch consisting of 0.05 mol L^{-1} TODGA in $[N_{1888}][NO_3]$ was prepared and split into two parts. One part was used in its water-saturated form and was irradiated as a single organic phase. The other part was irradiated in contact with an equal volume of 2.5 mol L^{-1} HNO_3. In the case of the soft-donor ligand, one batch composed of 0.01 mol L^{-1} $CyMe_4BTPhen$ in $[N_{1888}][NO_3]$ was prepared and split into two parts. One part was used in its water-saturated form and was irradiated as a single organic phase. The other part was irradiated in contact with an equal volume of 1.0 mol L^{-1} HNO_3. All irradiations were performed as static experiments.

2.4 Speciation studies with comparison of two ESI-MS methods

The radiolysis products are present in trace concentration in a highly charged matrix of the ionic liquid. For a higher reliability of results, a comparison of measurements was performed with two independent analytical instrumentations on the same irradiated sample series. The analyses were performed several days to several weeks after the gamma irradiation of the samples, thus only stable radiolysis products were detected.

UHPLC–ESI–am-MS measurements

Irradiated DGA samples in $[N_{1888}][NO_3]$ were diluted 1:10,000 in HPLC grade acetonitrile (Fisher Scientific) prior to analysis. The diluted samples were analyzed using a Thermo Scientific™ Vanquish™ UHPLC (ultra-high-performance liquid chromatograph) system consisting of a Vanquish F pump, Vanquish autosampler and Vanquish column compartment, coupled to a Thermo Scientific™ Q Exactive™ mass spectrometer (MS) equipped with a HESI-II probe electrospray-ionization-quadrupole - Orbitrap mass spectrometer with Xcalibur 4.0 software.

The chromatographic separation was achieved using a 5 µL injection onto a C18 reversed-phase column (Waters Acquity UPLC® BEH C18 2.1 × 100 mm, 1.7 µm). The column temperature was kept at 50 °C. The gradient elution program used a mobile phase A 10 mmol L^{-1} ammonium formate and 0.1 % formic acid in water:acetonitrile (1:1; *v/v*) and mobile phase B 2 mmol L^{-1} ammonium formate and 0.02 % formic acid in water:acetonitrile:isopropanol (2:10:88; *v/v*). The elution program was as follows: 0 – 4 min 65-40 % A; 4 – 12 min 40-15 % A; 12 – 16 min 15-0 % A; 16 - 16.1 min 0 – 65 % A; 16.1 – 20 min 65 % A, all at a flow rate of 400 µL min^{-1}.

The parameters of the mass spectrometer were as follows: Sheath gas flow rate 60 arbitrary units, aux gas flow rate 20 arbitrary units, ESI spray voltage 3.5 kV, capillary temperature 285 °C, aux gas heater temperature 370 °C. The experiments were done both in positive as in negative ionization mode with the following experimental conditions: scan range: *m/z* 200 – 1700, max injection time 200 ms, AGC target 1e^{6}, resolution 140,000. Data processing was performed using Thermo Scientific^{TM} Compound Discoverer^{TM} for easy peak finding, identifying the degradation products and identifying differences between samples. For the purpose of quantification, only the non-irradiated TODGA and CyMe$_4$BTPhen ligands and the [N$_{1888}$][NO$_3$] ionic liquid were available to construct calibration curves. From scoping studies it was known that the response factor of the ligand is dependent on the total ion concentration that reaches the detector (high cation concentration suppresses the signal intensity of the analyte). The total ion concentration reaching the detector depends on the amount of ionic liquid cation present in the injected sample. Thus to minimize matrix effects on the response function, matrix-matched calibration series were prepared from 0.05 mol L^{-1} TODGA in [N$_{1888}$][NO$_3$], from 0.01 mol $^{L-1}$CyMe$_4$BTPhen in [N$_{1888}$][NO$_3$], and from non-irradiated, water-saturated [N$_{1888}$][NO$_3$].

HPLC-ESI-MS/MS measurements

HPLC-ESI-MS/MS for quantification was performed with a Qtrap6500 instrument (ABSciex, Darmstadt) coupled with an Agilent 1260 HPLC system consisted of a binary pump system, an autosampler and a thermostatted column compartment. The MS parameters used for all methods were optimized by performing a Flow Injection Analysis (FIA) with standards and led to the following settings for all analyses: curtain gas (N_2) 40 arbitrary units (a.u.), temperature of the source 350 °C, nebulizer gas (N_2) 80 a.u., heater gas (N_2) 40 a.u and ion spray voltage (IS) 4500 V. Quantification after HPLC was performed using ESI-MS/MS detection in the multiple reaction-monitoring (MRM) mode in positive ionization mode. MRM transitions involving precursor ions $(M+H)^+$ and the two most abundant product ions were used for quantification of all analytes as shown in Table 1. All LC-MS/MS data acquisition and processing was carried out using the Software Analyst 1.6.1 (AB Sciex, Darmstadt). Quantification was performed with the Software Multiquant (AB Sciex, Darmstadt).

Table 1. Precursor and product ions used for quantification of TODGA and $CyMe_4BTPhen$

Parent molecule	Precursor ion (*m/z*)	Product Ion (*m/z*)	Declustering Potential DP (V)	Collision Energy (V)	Cell Exit Potential (V)
TODGA	581.4	312.3	11	45	24
TODGA	581.4	340.2	11	29	18
$CyMe_4BTPhen$	559.1	529.3	200	67	6
$CyMe_4BTPhen$	559.1	395.2	200	67	24

For TODGA, a Phenyl-X (100 × 4.6 mm; 2.6 µm particle size) column from Thermo Fisher was used with a gradient of 0.1 % formic acid in H_2O (A) and acetonitrile + 0.1 % formic acid (B) at 40 °C and a flow rate of 700 µL min^{-1}. The gradient is described in Table 2. The calibration was done using the non-irradiated TODGA samples by dilution. The linearity was found to be good in the region from 1 nmol L^{-1} to 50 nmol L^{-1} with $R^2 = 0.9995$ (Figure S 10). The variation coefficient of a 10 nmol L^{-1} standard of TODGA was 4.3 %.

Table 2. Applied elution gradient used during the chromatographic separation of TODGA

Run-time (min)	Composition (residual refers to A)
0 – 5	5% B
5 – 15	Increase to 90% B
15 – 20	90% B
20 – 20.5	Increase to 95% B
20.5 – 25	95% B
25 – 25.5	Decrease to 5% B
25.5 – 30	5% B

For $CyMe_4BTPhen$, a Gravity SB C18 (100 × 4.6 mm; 2.6 μm particle size) column from Phenomenex was used with an isocratic run of 2 % 0.1 % formic acid in H_2O (C) and 98 % methanol + 0.1 % formic acid (D) at 40 °C and a flow rate of 700 $\mu L\ min^{-1}$. The calibration was done using the non-irradiated $CyMe_4BTPhen$ samples by dilution. The linearity was found to be good in the region from 1 $nmol\ L^{-1}$ to 100 $nmol\ L^{-1}$ with $R^2 = 0.9997$ (Figure S11). The variation coefficient of a 10 $nmol\ L^{-1}$ standard of $CyMe_4BTPhen$ was 5.6 %.

3. Results and discussion

Samples irradiated in the water–saturated condition showed a significant coloration in function of the absorbed dose, while the color change in the case of the samples irradiated in the presence of an acidic aqueous phase was less expressed (Figure S1, S2). In order to probe the effect of irradiation on the solvents, both their solvent extraction properties and their chemical composition were studied with high-resolution mass spectroscopy before and after γ-irradiation. Two different analytical instruments (UHPLC-ESI-am-MS and HPLC-ESI-MS/MS) were used. The residual ligand concentration in the irradiated samples was quantified via a matrix-matched calibration series prepared from non-irradiated organic solution of TODGA (Figure S5, S10) or $CyMe_4BTPhen$ in $[N_{1888}][NO_3]$ (Figure S11).

3.1 Extraction studies on irradiated solvents

In order to study the effect of gamma irradiation on the extraction performance of the organic phase, batch solvent extractions were conducted using spiked aqueous feed solutions. Results of the batch solvent extraction studies using irradiated solvent composed of 0.05 mol L^{-1} TODGA in $[N_{1888}][NO_3]$ are shown in Figure 2. Results of the solvent extraction studies performed with irradiated solvent with an original composition of 0.01 mol L^{-1} $CyMe_4BTPhen$ in $[N_{1888}][NO_3]$ are shown in Figure 3.

Extraction studies with irradiated solvents containing TODGA

The distribution ratios of ^{241}Am, ^{244}Cm and ^{152}Eu when using the TODGA solvent irradiated in the absence of an acidic aqueous phase showed a decrease as a function of the absorbed dose (Figure 2 a). The extent of change in D values was about one order of magnitude in the case of ^{241}Am (11.9±1.6 → 1.6 ± 0.2), ^{244}Cm (19.6±3.1 → 1.7±0.3) as well as for ^{152}Eu (97.9±2.2 → 8.0±0.1). The change in distribution ratios did not cause a large change in separation factors (although they decreased slightly), suggesting that the decrease can be attributed to a decrease in ligand concentration. The $SF_{\mathrm{Cm/Am}}$ ranged from 2.1 to 1.1 over the entire investigated range, while the $SF_{\mathrm{Eu/Am}}$ varied between 8.7 and 5.2.

Initial distribution ratios of the three metal ions were higher in the case of samples that were irradiated in the presence of 2.5 mol L^{-1} HNO_3 (Figure 2 b) since the initial and equilibrium nitric acid concentrations were the same. In the case of samples irradiated without nitric acid (Figure 2 a), a part of HNO_3 was extracted reducing the equilibrium HNO_3 concentration in the aqueous phase compared to the initial concentration. In the case of irradiated samples in contact with nitric acid, the distribution ratios decreased more pronounced in the range of 0–1200 kGy absorbed dose compared to irradiated samples without contact with nitric acid. This indicates that the presence of nitric acid contributes to radiolysis of the ligand. At the highest absorbed dose the distribution ratios dropped by two orders of magnitude from their initial value obtained with non-irradiated organic phases: in the case of irradiated samples in contact with nitric acid ^{241}Am (22.5±3.5 → 0.63±0.08), ^{244}Cm (46.9±8.7 → 0.57±0.08) as well as ^{152}Eu (418±8 → 2.45±0.03).

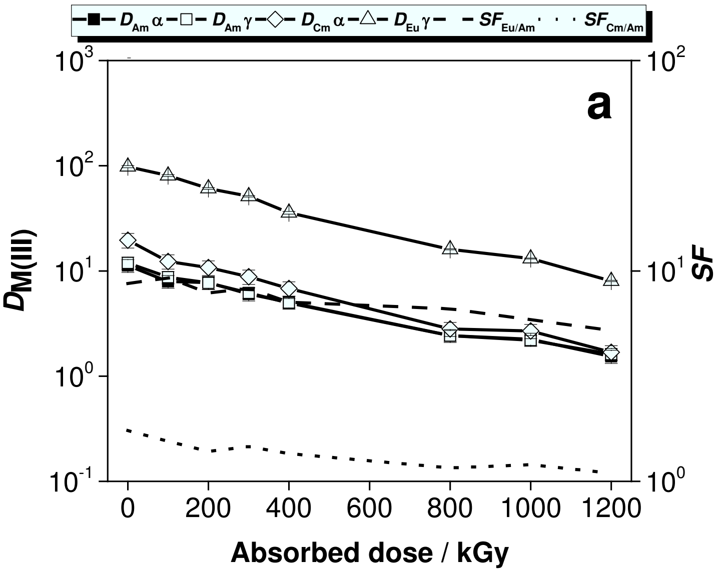

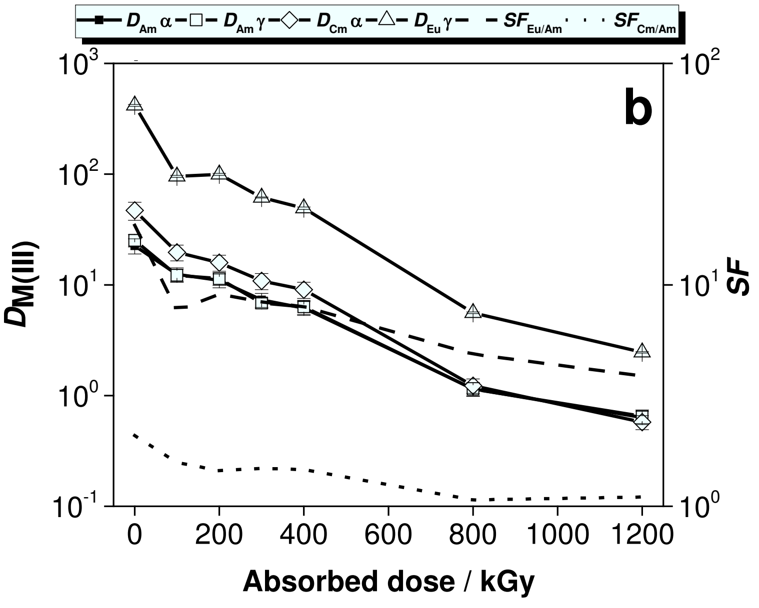

Figure 2. Distribution ratios of ^{241}Am (squares), ^{244}Cm (diamonds) and ^{152}Eu (triangles) as a function of absorbed dose. Samples irradiated with a ^{60}Co γ source in the absence of HNO_3 (a) or in contact with an equal volume of 2.5 mol L^{-1} HNO_3 (b). Org.: 0.05 mol L^{-1} TODGA in water-saturated $[N_{1888}][NO_3]$, Aq.: fresh 2.5 mol L^{-1} HNO_3, [Ln(III)] (La-Dy, Yb, Y) = 10^{-5} mol L^{-1} each, spiked with tracers of ^{241}Am, ^{244}Cm and ^{152}Eu, T = (22±1) °C at 2200 rpm for t = 2 h. The D_{Am} values determined with α and γ measurements overlap.

Extraction studies with irradiated solvents containing CyMe₄BTPhen

For the extraction studies using irradiated $CyMe_4BTPhen$ solvent without contact with nitric acid (Figure 3 a), the distribution ratios of Am (III), Cm(III) and Eu(III) went through a maximum and then decreased in function of absorbed dose up to 400 kGy: (^{241}Am (1000→ >>1000 → 440), ^{244}Cm (600→ 1000 → 475), ^{152}Eu (1.7 → 2.2 → 0.6). In former studies, a similar behavior was observed where solutions of $CyMe_4BTPhen$ or $CyMe_4BTBP$ in 1-octanol were irradiated in contact with 1 mol L^{-1} nitric acid solution.[24, 25] In the case of solvent irradiated in contact with nitric acid (Figure 3 b), the distribution ratios fluctuate and remained in the same order of magnitude over the entire investigated dose range of 400 kGy γ dose (^{241}Am (1000±200 → >> 1000), ^{244}Cm (600±100 → 500±100), ^{152}Eu (1.74±0.03 → 0.81±0.01)). The slight increase of distribution ratios with absorbed dose can be attributed to the formation of radiolysis products that are even better extractants for trivalent minor actinides than the original ligand, as postulated by Schmidt *et al.* [24, 25] In their irradiation studies using 1-octanol diluent for either $CyMe_4BTPhen$ or $CyMe_4BTBP$ ligands, nitric acid showed a protective effect, and it was hypothesized that nitric acid scavenges the radicals formed from the diluent.[24, 50] The same protective effect of nitric acid during irradiation was observed for C5-BPP (another N-donor extractant) in 1-octanol.[26] Kondé *et al.*, found that the radiation stability of $CyMe_4BTPhen$ in FS-13 diluent is lower in the presence of an aqueous phase containing 1 or 2 mol L^{-1} HNO_3 during irradiation, compared to samples irradiated in contact with water.[27] In that study, the authors found an increase in Am(III) and Eu(III) distribution ratios as a function of absorbed dose in a solution composed of 0.005 mol L^{-1} $CyMe_4BTPhen$ in FS-13.[27] The authors also concluded that the increase in *D* values was caused by the formation of degradation products that were stronger extractants than $CyMe_4BTPhen$ itself. The possible composition of such degradation products was not identified. Interestingly, the chemically similar $CyMe_4BTBP$ in the same diluent seemed to be fairly unaffected by the radiation.

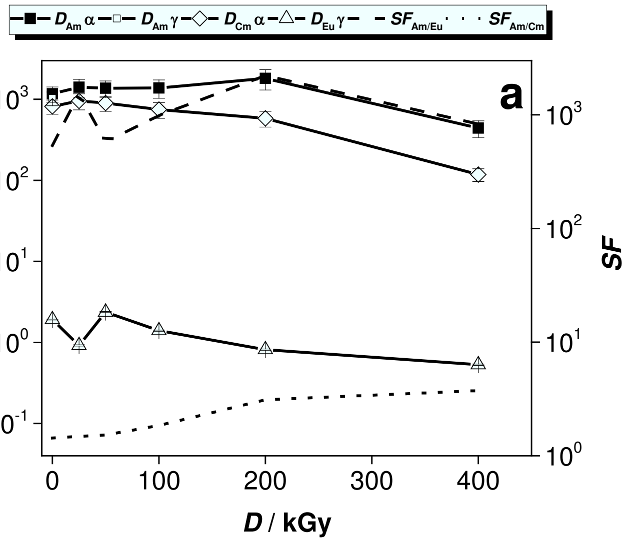

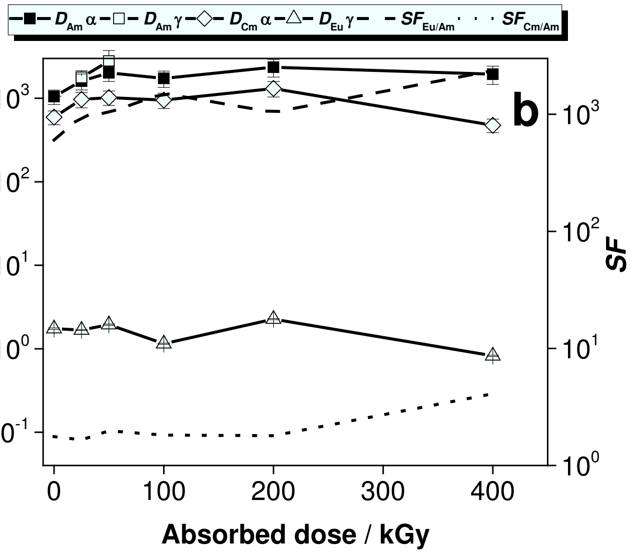

Figure 3. Distribution ratios of ^{241}Am (squares), ^{244}Cm (diamonds) and ^{152}Eu (triangles) as a function of absorbed dose. Organic phase: 0.01 mol L^{-1} CyMe$_4$BTPhen in [N$_{1888}$][NO$_3$] irradiated in the absence of HNO$_3$ (a) and in contact with an equal volume of 1 mol L^{-1} HNO$_3$ (b) with a ^{60}Co γ – source; aqueous phase: $[HNO_3]_{ini.}$ = 1 mol L^{-1}, traces of ^{241}Am, ^{244}Cm and ^{152}Eu and stable Ln(III)-ions (La-Dy, Yb, Y) at a concentration of 10^{-5} mol L^{-1}. Samples were equilibrated at (22±1) °C by shaking at 2200 rpm for 8.5 h.

3.2 Degradation of the [N$_{1888}$]$^+$ cation

During UHPLC – ESI –-MS measurements, the [N$_{1888}$]$^+$ cation (*m/z* = 368.42) eluted with a retention time of 1.94 min, and was seen as the most intense peak in the positive ionization mode. The evolution of this compound's signal intensity as a function of absorbed dose is shown in Figure 4. The radiolysis of the [N$_{1888}$]$^+$ cation resulted in a progressive decrease of the peak area as a function of absorbed dose. At 1.2 MGy absorbed dose, the total loss in peak area compared to that of the original peak area is ca. 10 % and 17 % under the neutral or the acidic conditions, respectively.

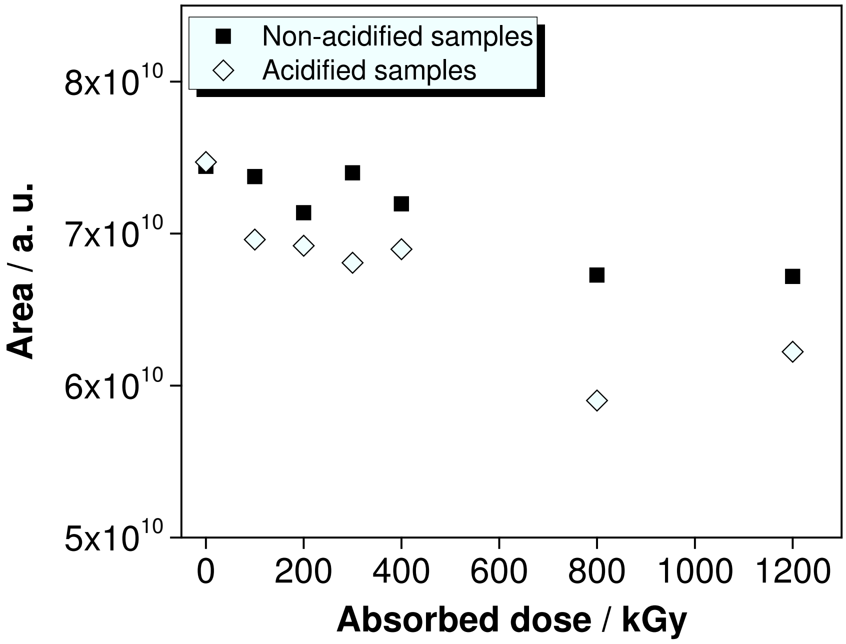

Figure 4. Plot of blank-corrected peak areas vs. absorbed dose for the compound with *m/z* = 368.42 (identified as the $[N_{1888}]^+$ cation).

3.3 Identification of the radiolysis products of $[N_{1888}]^+$ cation

Prior to analyzing irradiated solvents containing either TODGA or $CyMe_4BTPhen$, the degradation products of $[N_{1888}][NO_3]$ were identified by supposing bond cleavage reactions followed by a substitution reaction in place of the cleaved bond and chemical functionalization of the parent $[N_{1888}]^+$ cation or its degradation products. Figure 5 provides a non-exhaustive list of identified compounds, for which the measured mass-to-charge (*m/z*) ratios correspond well with the theoretical *m/z* ratios. Table S2 gives an overview of identified species that could be formed from the ionic liquid during irradiation. Compounds listed in Figure 5 are derived from the data obtained using positive ionization mode. In the negative ionization mode, only one peak was detected with a retention time of 2.58 min and *m/z* = 459.43. The structure of the latter species could not be identified.

The diluent radiolysis yielded compounds that can be grouped into three broad categories: (1) chemically functionalized radiolysis products of the parent cation (hydroxylated, carboxylated or nitrosylated derivatives) and products formed via hydrogen abstraction, (2) products formed as a result of dimerization and (3) products formed as a result of N-C_{alkyl} bond cleavage in the $[N_{1888}]^+$ cation. The presence of structural isomers can be an explanation for the presence of more than one distinct elution peak for compounds with identical *m/z* values. From the relative intensities and retention times it is not possible to determine the exact location of the functional group in a mixture of geometrical isomer structures. A quantitative determination of the concentration of each compound would require the synthesis of calibration standards of each compound, followed by checking their identity on the basis of their retention times in the HPLC column under the same conditions as used for the analysis of irradiated samples. Such an extensive organic synthesis work and iterative HPLC analysis was outside the scope of this project. In the absence of calibration standards, the radiolysis products of the diluent cation and the dissolved ligand were qualitatively analyzed.

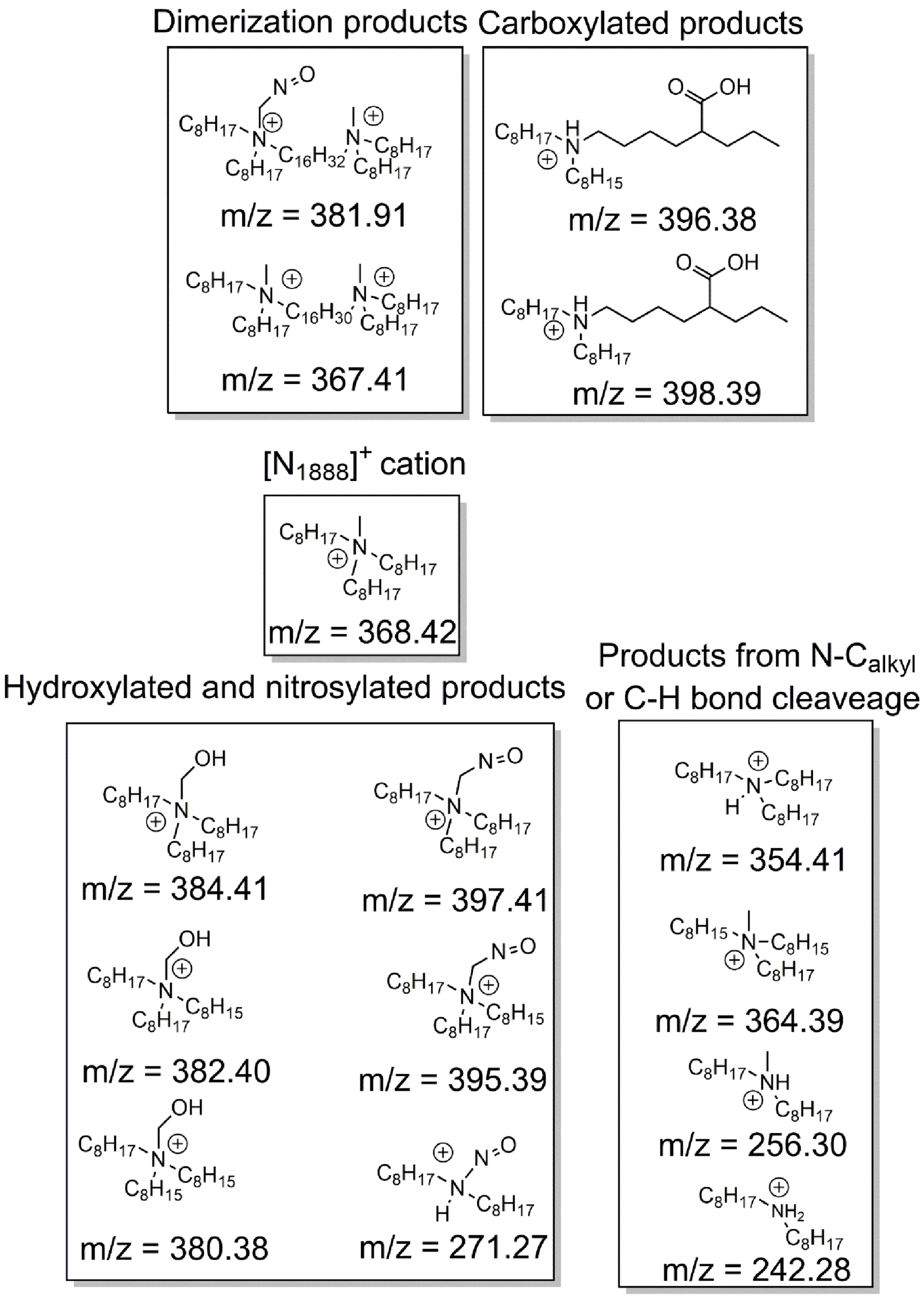

Figure 5. Tentative structures of radiolysis products formed from the $[N_{1888}]^+$ cation and measured *m/z* ratios in UHPLC-ESI-am-MS analysis.

Radiolysis products formed as a result of N-C_{alkyl} or C-H bond rupture

The peak with a short retention time (RT = 0.96-0.98 min) in the chromatogram of irradiated [N_{1888}][NO_3] belongs to a species with a *m/z* = 256.299 This mass-to-charge ratio corresponds well with *N*-methyl-di-*n*-octylammonium cation which could be formed from the parent cation by cleavage of one N-C_{octyl} bond. This type of covalent bond is weaker than the C-C or C-H bonds. A second peak with identical *m/z* = 256.264 value and a retention time of 2.29 min can be the indication of the presence of two species in the irradiated samples. The N-C_{methyl} bond cleavage could yield either tri-*n*-octylamine or tri-*n*-octylammonium-ion. Two species with retention times 1.8 min and 2.3 min were found with nearly identical *m/z* = 354.4106 and *m/z* = 354.4096, respectively), which could be correspond with tri-*n*-octylamine (protonated in the ion source) and tri-*n*-octylammonium.

Radiolysis products formed via a chemical functionalization or oxidation of the [N_{1888}]$^+$ cation or one of its radiolysis products

Several nitroso functionalized species were formed from the [N_{1888}]$^+$ cation. The presence of several overlapping peaks suggests that these compounds are structural isomers, where the functional group is located at different carbon atoms. All of these species were eluted with retention times ranging from 1.5 – 2 min (*m/z* = 397.41). These species were not present in non-irradiated samples, and were created in a high abundance, but almost exclusively in the non-acidified samples. Figure S3 shows the build-up of this compound under the effect of absorbed γ-radiation. A compound with a retention time 0.96 min (*m/z* = 395.39), could be derived from the species with *m/z* = 397.41, supposing a H-abstraction reaction. Nitrosylated species are supposed to be responsible for the progressive coloration of non-acidified samples with dose (Figures S1 and S2). None of the other (tentatively) identified compounds have a functional group that is expected to have a high absorption in the visible spectrum of light. A compound eluting with a 4.21 min retention time belongs to a compound with *m/z* = 271.27 that could be attributed to a protonated *N*-nitroso-*N,N*-dioctylamine. The explanation for the marked difference in color and in the measured abundance of certain radiolysis products between acidic and neutral samples could be related to the difference in relative abundance of primary radiolysis products of water ($^{\bullet}OH$ and e_{aq}^{-}) and the reactivity of HNO_3 and NO_3^- with $^{\bullet}OH$-radicals. From previous studies it is known, that a quaternary ammonium salt (tetrabutyl ammonium nitrate) generates $^{\bullet}NO_3$ radicals when the solvent is exposed to ionizing radiation.[51] $[N_{1888}][NO_3]$ only differs in the alkyl chain length from tetrabutyl ammonium nitrate, thus it can be expected that radiation will generate $^{\bullet}NO_3$ radicals in the organic phase too.

Under highly acidic conditions, the main species present in aqueous solutions is $^{\bullet}OH$. Nitric acid at pH = 0 is known to scavenge hydroxyl radicals rapidly according to equation (3) while generating nitrate radicals.[52]

$$\mathrm{HNO_3 + OH^{\bullet} \rightarrow NO_3^{\bullet} + H_2O} \qquad (3)$$

The nitrate radical produced in reaction (4) or generated from the diluent is known to react slowly with saturated hydrocarbons via H-abstraction mechanism and via electrophilic addition to alkenes.[53] Thus in principle, there are nitrate radical production pathways under both irradiation conditions, however, these nitrate radicals did not generate stable nitrated organic radiolysis products at high abundance in the ionic liquid under neither acidic nor neutral conditions.

In contrast, the samples irradiated under neutral conditions yielded nitrosylated organic compounds. Based on the above considerations, the source of the NO functional group is not nitrate radicals, but another reaction mechanism. These are obtained most probably as a result of several successive radical reactions. At higher pH, the most abundant radiolysis product in water is solvated electron. The solvated electrons can be attracted by the cations of the ionic liquid or react with NO_3^- ions and generate nitrite radicals and nitrite anions (reactions 4-6). The reaction between solvated electron and nitrate anion is known to have a very fast reaction rate $k = 9.7 \times 10^9$ mol L^{-1} s^{-1}).[54] The reaction rate of dinitrogene tetraoxide with water is relatively slow ($k = 1.5 \times 10^3$ mol L^{-1} s^{-1}) suggesting that under the conditions of the irradiation, nitrite radicals should be abundant, while solvated electrons are probably present at low concentrations. Nitrite anions can also scavenge solvated electrons (reaction 7) and eventually result in the formation of nitroso-compounds (reaction 8).[55, 56] However, based on the considerations of abovementioned known reaction rates, it is probably the reaction of nitrite radicals with the cations of the quaternary ammonium cations that generate nitrosylated compounds (reaction 9)

$$\mathrm{NO_3^- + e^-_{aq.} + H_2O \rightarrow NO_2^\bullet + 2OH^-} \tag{4}$$

$$\mathrm{2\,NO_2^\bullet \rightarrow N_2O_4} \tag{5}$$

$$\mathrm{N_2O_4 + H_2O \rightarrow NO_2^- + NO_3^- + 2H^+} \tag{6}$$

$$\mathrm{NO_2^- + e^-_{aq.} \xrightarrow{H_2O} NO + 2OH^-} \tag{7}$$

$$\mathrm{R^\bullet + NO \rightarrow R - NO} \tag{8}$$

$$\mathrm{[R_3N - CH_3]^+ + NO_2^\bullet \rightarrow [R_3N - CH_2 - NO]^+ + OH^\bullet} \tag{9}$$

A species with *m/z* = 384.41 was found to be present as one of the most abundant degradation products (identified as $C_{25}H_{54}NO^+$). The selected ion chromatogram showed the presence of six, well resolved peaks with retention times from 1.5 – 2 min. Five of the peaks had nearly the same intensity, while one had only half of the intensity of the rest of the peaks. The presence of six isomers suggest that there are multiple sites available for substitution (e.g. five on the octyl chains: C_8 to C_3 while the sixth compound could be one with substitution on the methyl group). The resulting products have slightly different affinity for the column, that resulted in the separation of their elution times. This compound is tentatively associated as a product formed from the parent $[N_{1888}]^+$ cation via a hydroxylation reaction. Formation of a sodium-containing adduct in the ion source of these hydroxyl-group modified structures can be an explanation for the presence of the species with m/z = 407.43, eluting with a retention time of 1.25 min. A hydroxylation reaction leading to the formation of the species with m/z = 384.41 might have also taken place on the various families of degradation products and could be responsible for the species with m/z = 382.40 and 380.38. The water content of the reverse micelles present in the organic phase could have served as a source of $^{\bullet}OH$ radicals in the hydroxylation reaction, as $^{\bullet}OH$ radicals are main radiolysis products of water radiolysis.[54] Species eluting with a retention time of 1.5 – 1.6 min (m/z = 364.39), as well as with retention times of 1.76 min (m/z = 366.41) were found in the irradiated $[N_{1888}][NO_3]$ samples. These species are possibly oxidation products from H_2 elimination with the formation of one or two double bonds (or ring closures) in the alkyl chains of the tri-*n*-octylmethylammonium cation. The peak areas of the species with m/z = 366.41 gave signals with roughly a factor of 10 times higher signal intensity than the species which are associated with two double bonds. The hydrogen atom cleavage is therefore possibly occurring in a consecutive way.

Under both neutral and acidic irradiation conditions, two additional compounds were formed from the $[N_{1888}]^+$ cation, which were identified as carboxylated derivatives: m/z = 398.39 and 396.38 with short retention times (0.91 and 0.95 min, respectively).

Radiolysis products formed via dimerization of $[N_{1888}]^+$ cation

A very broad signal with the highest intensity at a retention time of 2.90 min has a mass to charge ratio of 367.41 (isotopic sub-peaks separated from each other by 0.5 amu). This species (identified as a doubly charged compound with a composition: $C_{50}H_{104}N_2^{2+}$) is clearly belonging to the diluent, and cannot be associated to the formation of a double structure in the ion source, since the elution occurs separately after the diluent peak. Such high molar mass indicates that two cations underwent a dimerization reaction. Similar recombination reactions of alkyl chains in *n*-dodecane under the effect of γ radiation have formerly been described in the literature.[57] Since numerous combination possibilities exist for the recombination to take place, it is expected that these double structures form a large mixture of isomeric structures, with slightly different elution behavior, which could explain the broad peak shape. A species that could be identified as a nitrosylated dimer formed from $[N_{1888}]^+$ cation (*m/z* = 381.91, with isotopic sub-peaks separated from each other by 0.5 amu) eluted with a retention time 2.4 min. Similarly to the case of other nitrosylated compounds, it was only formed at high abundance in the neutral, non-acidified samples.

3.4 Degradation of TODGA

Residual ligand concentration was determined via the use of two independent analytical methods (UHPLC-ESI-am-MS and HPLC-ESI-MS/MS respectively). A calibration curve for the ligand was constructed using a dilution series prepared from non-irradiated solution of 0.05 mol L^{-1} TODGA in $[N_{1888}][NO_3]$ (Figure S5 and S10). The dose constant for the two systems was calculated by linear regression of the natural logarithm of the ratio of residual and initial TODGA concentrations vs. absorbed dose (see Figure 6 and Table 3). Mincher and Curry have shown that this dose constant, *d*, is the most appropriate figure-of-merit for most radiolysis studies, where trace components are dissolved in a bulk diluent.[58] For many systems, the plot of ligand/analyte concentration vs. absorbed dose is best fitted with an exponential curve, as in equation (10):

$$C = C_o e^{-dD} \tag{10}$$

where C is the concentration of the analyte at a given absorbed dose, C_o is the initial concentration of the analyte, d is the dose constant, and D is the absorbed dose. The higher the dose constant, the higher radiation sensitive the compound is.

The ln[C_{TODGA}/C^0_{TODGA}] vs. absorbed dose plots determined from the UHPLC-ESI-am-MS measurements show a linear trend over the entire 0 – 1200 kGy dose range (Figure 6a). The observed (9.10 ± 0.72) × 10^{-4} kGy^{-1} dose constant for TODGA in [N_{1888}][NO_3] is more than three times lower than that determined for TODGA in *n*-dodecane by Sugo *et al.*[14] or by Zarzana *et al.*[17] and five times lower than the dose constant of Me-TODGA determined by Galán *et al.*[50] The dose constant of TODGA in the case of the acidified samples was slightly larger ((1.17 ± 0.13) × 10^{-3} kGy^{-1}), indicating that the irradiation in the presence of nitric acid resulted in a slightly higher degradation rate of TODGA, compared to the samples irradiated under neutral conditions as a single organic phase. The analysis of TODGA-containing samples with the UHPLC-ESI-MS/MS method was restricted to the absorbed dose range of 0-800 kGy, as the ligand concentrations for 1000 and 1200 kGy absorbed dose were found to be higher than in the sample of 800 kGy (attributed to a measurement artefact). The results showed similar, but slightly higher dose constant values as compared with the other method for TODGA under neutral and acidic irradiation conditions: (1.12 ± 0.26) × 10^{-3} kGy^{-1} and (1.50 ± 0.15) × 10^{-3} kGy^{-1}, respectively (Figure 6b). The comparison of the residual ligand concentration measurement with two different analytical instrumentations provided similar dose constants, and both suggested a higher degradation rate for TODGA under acidic conditions.

Roscioli-Johnson *et al.* did not find differences in radiolysis rates for *N*,*N*-di-dodecyl-*N'*,*N'*-di-octyldiglycolamide (D^3DODGA) dissolved in *n*-dodecane diluent where the samples were irradiated up to 400 kGy with or without the presence of an aqueous acidic phase.[59] They did however find differences in the relative abundance of various radiolysis products formed from the ligand. Similarly, Zarzana *et al.* also found no significant effect on the apparent degradation rates of TODGA or T(EH)DGA under neutral or acidic conditions (up to 400 kGy absorbed dose).[17]

The explanation of a higher radiation stability of TODGA in $[N_{1888}][NO_3]$ ionic liquid compared to that found previously in *n*-dodecane under both acidic and neutral conditions can be caused by the differences in chemical composition of the solvents, their supramolecular organization and/or viscosity.

As far as the chemical composition is concerned, a high nitrate ion concentration is present in $[N_{1888}][NO_3]$. Since this ionic liquid is a good extractant for nitric acid,[33] a high nitric acid concentration is also ensured in the organic phase in bi-phasic irradiations. As suggested above in reactions 4-8 nitric acid and nitrate anions are good scavengers of $^{\bullet}OH$ and e_{aq}^{-}.

Besides the obvious chemical differences between a TODGA in *n*-dodecane solution and TODGA in $[N_{1888}][NO_3]$ solution, there are also differences between their supramolecular organizations that can affect the fate of primary radiolysis products. TODGA in *n*-dodecane doesn't form an ideal solution, instead such solutions show microheterogeneities due to the surfactant property of TODGA. Above the critical micelle concentration (0.1 mol L^{-1}) they form reverse micelles with an average diameter of 2.8 nm.[60] The ligand molecules are enriched and oriented towards the aqueous/organic interphase with the oxygen donor atoms - irrespective whether the water is present in a bulk phase or in small hydrophilic pockets enclosed in reverse micelles comprised of four TODGA molecules. In the case of the $[N_{1888}][NO_3]$ ionic liquid, the diluent itself has a supramolecular organization, forming aggregates the average size of which increase upon addition of DGA ligands (~ 12 nm → ~25 nm) and decrease with increase of extracted nitric acid or metal ion concentration (~ 27 nm → < ~ 10 nm).[35] The average size of these aggregates is one order of magnitude larger than those reverse micelles comprised exclusively of TODGA tetramers. One explanation for the larger aggregates in the ionic liquid can be that the highly polar ion pairs stabilize large reverse micelles, where the anion and the polar head of the quaternary ammonium ion are pointing towards an aqueous core. Moreover, the increase of aggregate size with ligand concentration suggest that the ligands form part of these aggregates or mixed reverse micelles. Such supramolecular organization of the diluent can contribute to the apparently lower degradation rate of TODGA. The ionic liquid cations attract solvated electrons formed in the aqueous phase, reducing the probability of their interaction with TODGA.

When the energy of radiation is deposited in an aliphatic organic phase, carbon-centered radicals are formed that enter into charge transfer reactions with TODGA molecules. Such radical formation can be expected from the *n*-octyl chains of $[N_{1888}]^+$ cations and their reaction with TODGA molecules is depending on the diffusion through the bulk phase. As the diffusion is significantly hindered due to the high viscosity and the presence of large aggregates of the ionic liquid, the radicals have a higher chance of recombination before reacting with a solute.

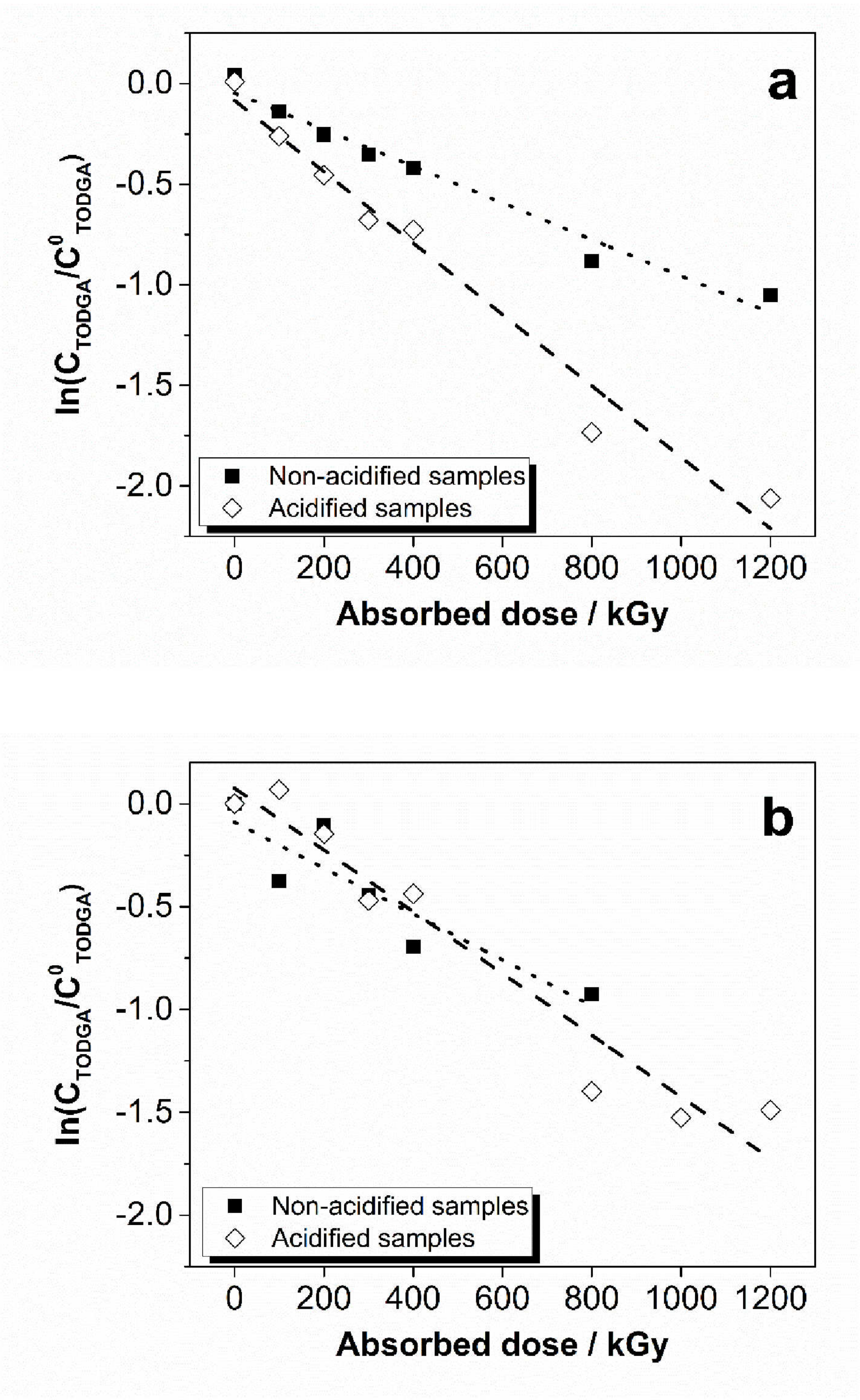

Figure 6. Natural logarithm of the ratio of final and initial TODGA concentration as a function of absorbed dose, determined by UHPLC-ESI-am-MS (a) and HPLC-ESI-MS/MS methods (b).

Table 3. Dose constants determined from the ln[C_{TODGA}/$C^0{}_{TODGA}$] vs. absorbed dose plots with two different methods.

Composition	Dose constant *d* (kGy^{-1}) (UHPLC-ESI-am-MS)	Pearson's Correlation coefficient	Dose constant *d* (kGy^{-1}) (HPLC-ESI-MS/MS)	Pearson's Correlation coefficient
0.05 mol L^{-1} TODGA in [N_{1888}][NO_3]	(9.10 ± 0.72) × 10^{-4}	-0.98464	(1.12 ± 0.26) × 10^{-3}	-0.90519
0.05 mol L^{-1} TODGA in [N_{1888}][NO_3] + 2.5 mol L^{-1} HNO_3	(1.17 ± 0.13) × 10^{-3}	-0.98668	(1.50 ± 0.15) × 10^{-3}	-0.9709

3.5 *Identification of TODGA radiolysis products*

The analysis focused on the confirmation of the presence of degradation products that were identified in former studies on irradiated organic solutions of TODGA or its analogs in molecular diluents.[15-17, 59] Our study confirmed the presence of all decomposition products that were formerly identified by Galàn *et al.*[15, 16], Zarzana *et al.*[17] and Roscioli-Johnson *et al.*[59] suggesting that the decomposition reactions of various diglycolamides (DGAs) follow a similar pathway (bond-cleavage within the diglycolamide core and de-alkylation) as in *n*-dodecane. The formerly suggested degradation scheme for DGAs is presented on the example of TODGA in Figure 7.

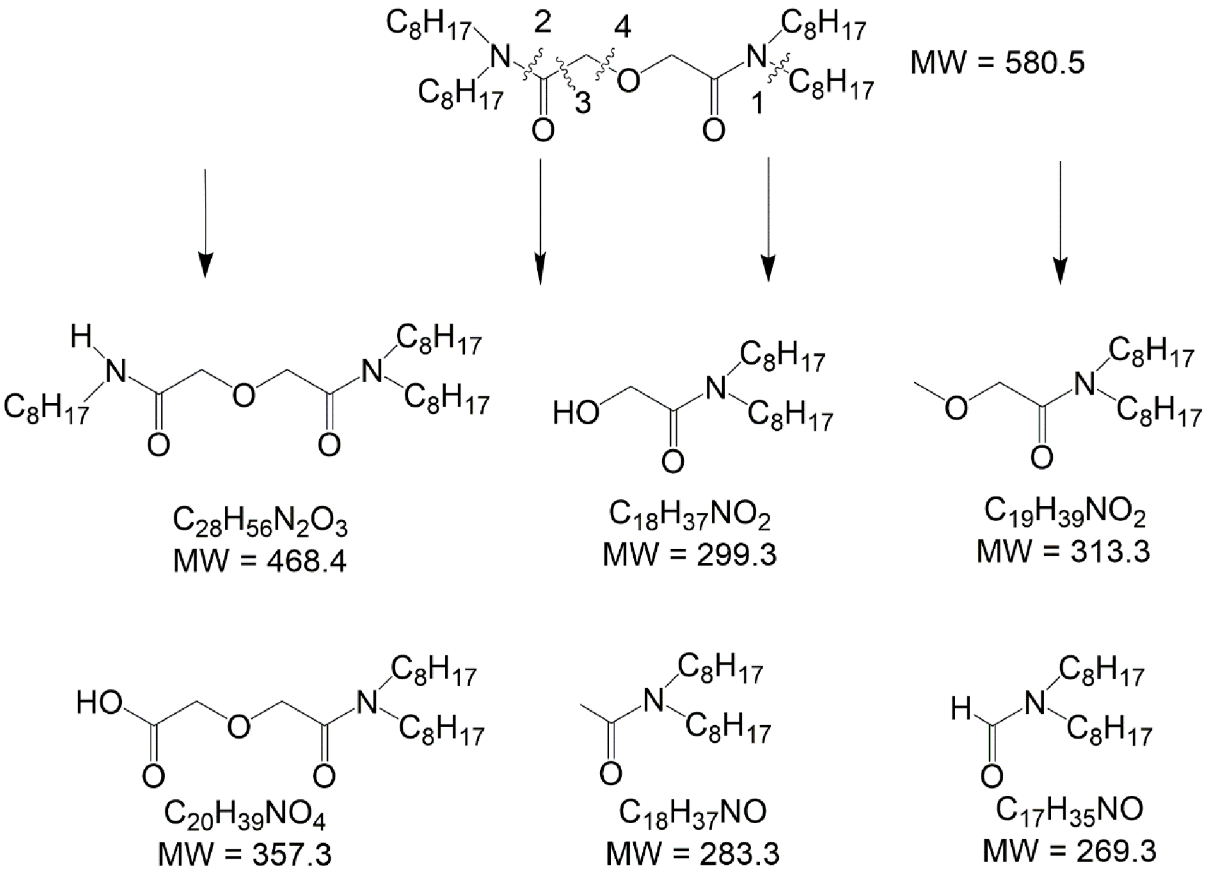

Figure 7. Scheme of the bond cleavage on TODGA exposed to gamma radiation and a tentative assignment of degradation products (MW representing the monoisotopic molar weight of the compounds).

As depicted in Figure 7 there are four possibilities for bond rupture within the symmetric DGA core: cleavage of C_{alkyl}-N (1), cleavage of N-$C_{carbonyl}$ (2), cleavage of $C_{carbonyl}$-$C_{methylene}$ (3), and cleavage of $C_{methylene}$ – O_{ether} bond (4). From theory, it is known, that the strength of these bonds follow the order of C-N (293 kJ mol^{-1}) < C-C (347 kJ mol^{-1}) < C-O (358 kJ mol^{-1}).[61] Cleavage of bond (1), followed by the addition of a hydrogen atom to the fragments would result in an octane molecule (MW = 114) and *N*,*N*,*N’*-tri-*n*-octyl diglycolamide (MW = 468.43).

Our analysis of the TODGA degradation products showed that change of *n*-dodecane to another diluent can provide a lower degradation rate, but has little influence on degradation pathways for TODGA. This finding suggest that the dissociative de-excitation of TODGA molecules upon reacting with a primary radiolysis product cannot be avoided nor altered, $[N_{1888}][NO_3]$ can nonetheless scavenge more efficiently reactive species than *n*-dodecane. The relative abundance of the radiolysis products under the two irradiation conditions (Figures S6-S9) were considerably different. In samples irradiated under neutral conditions, typically higher peak areas were found for all (tentatively) identified radiolysis products. The only exception was 5-(*N,N*-dioctyl)amido-3-oxopentanoic acid, which was more abundant in samples irradiated under acidic conditions. The apparently higher signal intensities recorded during the ESI-MS measurement performed after the irradiation do not necessarily mean a higher formation rate. It is equally possible, that only the primary radiolysis products themselves were less stable in the presence of an acidic aqueous phase.

3.6 Degradation of $CyMe_4BTPhen$

Quantification of the residual ligand concentration was more challenging in the case of the $CyMe_4BTPhen$ containing samples, as this ligand had a tendency to co-elute from the chromatographic column with the cation of the ionic liquid. The high concentration of these charged particles prevented the quantification of the ligand via the UHPLC-ESI-am-MS method. In the case of the HPLC-ESI-MS/MS method, a linear calibration curve was obtained (Figure S11). The residual ligand concentration as a function of the absorbed dose is plotted in Figure 8.

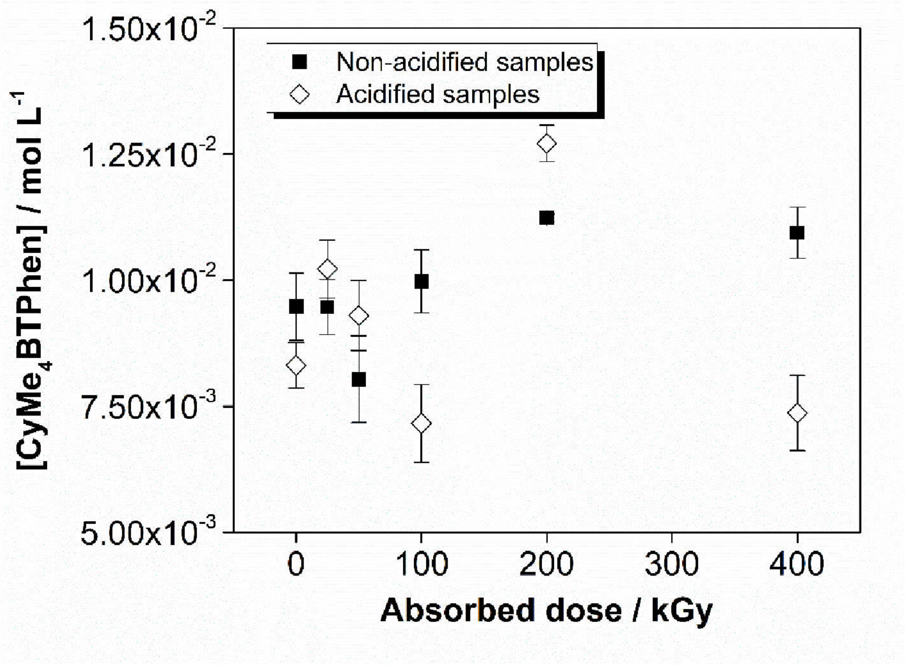

Figure 8. The residual CyMe$_4$BTPhen ligand concentration as a function of absorbed dose, initial composition: 0.01 mol L^{-1} CyMe$_4$BTPhen in [N$_{1888}$][NO$_3$].

In the samples irradiated to 25 - 400 kGy absorbed dose under neutral conditions, the residual ligand concentration was statistically not different from the initial ligand (0.01 mol L^{-1}) concentration. In case the main radiolysis product is an adduct formed between the ionic liquid cation and the ligand, the observed ligand concentration might be apparently unaltered compared to the original ligand concentration, if they co-elute from the chromatographic column and break down into the original constituting species in the ion source. Thus we rather not make conclusions on ligand degradation.

In a formerly performed radiation stability study using 1-octanol as a diluent only ~ 5 % of the original ligand concentration was preserved after 100 kGy absorbed dose.[25] In phenyl trifluoromethyl sulfone (FS-13) diluent, Kondé *et al.* have found that the residual CyMe$_4$BTPhen concentration after 100 kGy absorbed dose in the absence of HNO$_3$ during irradiation was (68.6±1.2) % of the original.[27]

3.7 Identification of CyMe$_4$BTPhen radiolysis product and its behavior as a function of absorbed dose

The chemical speciation performed on the irradiated solvents composed of 0.01 mol L^{-1} CyMe$_4$BTPhen in [N$_{1888}$][NO$_3$] by UHPLC-ESI-am-MS method indicated the presence of only one compound (*m/z* = 462.87, RT = 4.00 min), that could be identified as a radiolysis product of CyMe$_4$BTPhen. The mass-to-charge ratio of this species suggests that it is a protonated, doubly charged adduct formed between the ligand CyMe$_4$BTPhen and the [N$_{1888}$]$^+$ cation. No other species found in the spectra could be assigned as a degradation product formed from the ligand (Table S3); all the other species were attributed to the diluent and its radiolysis products. The absence of other ligand radiolysis product in the mass spectra does not exclude the existence of other degradation pathways, but the products of such reactions are either not stable enough themselves or not created in high enough concentration to be detectable under the applied conditions. Figure 9 shows the plot of the recorded peak areas vs. absorbed dose under neutral and acidic conditions. The compound was not present in the non-irradiated samples. At low absorbed doses, the production rate in samples irradiated in acidic conditions was higher than under neutral one-phase irradiation conditions.

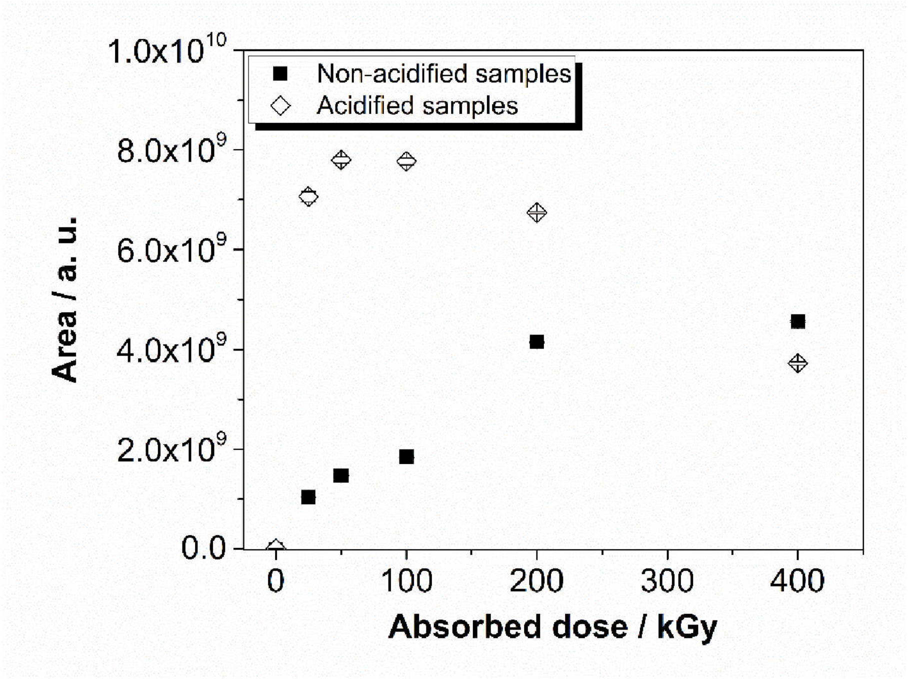

Figure 9. Plot of blank-corrected peak areas vs. absorbed dose for the doubly charged species with m/z = 462.87 (tentatively identified as an adduct formed between $CyMe_4BTPhen$ and the $[N_{1888}]^+$ cation).

Figure 10 shows one possible compound structure formed as an adduct between the ligand and the cation of the diluent. This structure is based on the assumption that the binding cavity of the molecule is left intact, and substitution occurs mainly on the 1,10-phenanthroline backbone.

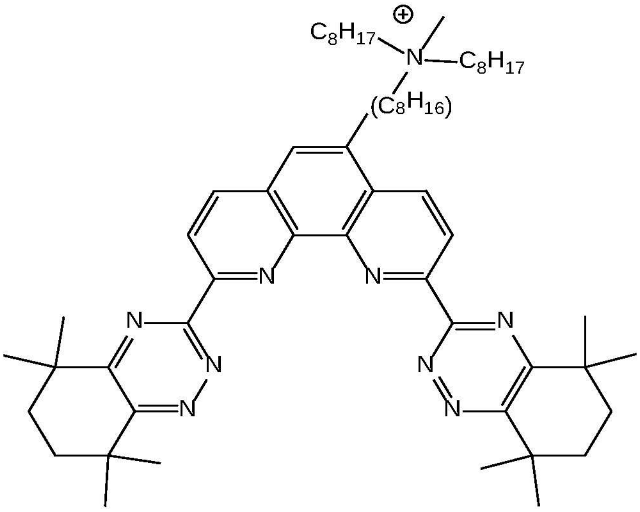

Figure 10. Tentative chemical structure of the adduct formed between the $[N_{1888}]^+$ cation and $CyMe_4BTPhen$ (chemical formula: $C_{59}H_{90}N_9$, measured m/z = 462.87).

4. Conclusions

The radiolytic stability of solvents composed of i) 0.05 mol L^{-1} TODGA and ii) 0.01 mol L^{-1} $CyMe_4BTPhen$ in the ionic liquid diluent $[N_{1888}][NO_3]$ irradiated by a ^{60}Co gamma source were studied by both solvent extraction and chemical analysis using the UHPLC-ESI-am-MS and HPLC-ESI-MS/MS methods. The observed trend for the distribution ratios of trivalent minor actinides and Eu(III) showed a steady decrease as a function of absorbed dose in the case of the TODGA solvent. The presence of an aqueous phase containing nitric acid during irradiation resulted in a different relative abundance of most radiolysis products formed from TODGA or the ionic liquid. Chemical analysis revealed that the degradation pathways of TODGA in $[N_{1888}][NO_3]$ ionic liquid are similar to those identified in *n*-dodecane: de-alkylation reactions and bond cleavage within the DGA core, followed by H addition were discerned from the proposed structures of the radiolysis products. The dose constant for TODGA in $[N_{1888}][NO_3]$ diluent under neutral or acidic irradiation conditions were $(9.10\pm0.72) \times 10^{-4}$ kGy^{-1} and $(1.17\pm0.13) \times 10^{-3}$ kGy^{-1}, respectively, in the 0 – 1200 kGy dose range. These dose constants were nearly four times lower than the values determined for lipophilic DGAs in *n*-dodecane using similar gamma energies, dose rates and absorbed doses. This finding suggests that $[N_{1888}][[NO_3]$ diluent scavenges the reactive radicals more effectively than *n*-dodecane, but the change in diluent doesn't cause a fundamental change in the dissociative de-excitation of the ligand. The dose constants for $CyMe_4BTPhen$ in the $[N_{1888}][NO_3]$ diluent under neutral or acidic irradiation conditions could not be determined. The distribution ratios slightly increased under the effect of absorbed dose, indicating the formation of a radiolysis product(s) that are efficient extractants as well. The cation of the ionic liquid diluent underwent multiple reactions under the effect of gamma radiation yielding nitrosylated, carboxylated and hydroxylated derivatives, isomers containing double bonds, as well as dimers and compounds with cleavages in the alkyl chains.

5. Acknowledgement

The authors would like to thank Andrei Goussarov, Steven Van Loven and Kris Thys from the BEX unit for performing the γ irradiations. P. Z. acknowledges the SCK•CEN Academy for providing funding for a PhD fellowship and the FOD Economie for providing additional support via the Energietransitiefonds. The authors would like to thank Magda Ooms for the help with the alpha measurements and Prisca Verheyen for the help with the ICP-MS measurements.

6. References

Uncategorized References

[1] *Homogeneous versus Heterogeneous Recycling of Transuranics in Fast Reactors,* NEA 7077, OECD-NEA, **2012**.

[2] *Potential Benefits and Impacts of Advanced Nuclear Fuel Cycles with Actinide Partitioning and Transmutation,* NEA 6894, OECD-NEA, **2011**.

[3] Poinssot, C., Bourg, S., Boullis, B., Improving the nuclear energy sustainability by decreasing its environmental footprint. Guidelines from life cycle assessment simulations*, Prog. Nucl. Energ.* **2016**, *92*, 234-241.

[4] Poinssot, C., Bourg, S., Ouvrier, N., Combernoux, N., Rostaing, C., Vargas-Gonzalez, M., Bruno, J., Assessment of the environmental footprint of nuclear energy systems. Comparison between closed and open fuel cycles.*, Energy* **2014**, *69*, 199-211.

[5] Geist, A., Taylor, R., Ekberg, C., Guilbaud, P., Modolo, G., Bourg, S., The SACSESS Hydrometallurgy Domain — An Overview*, Procedia Chem.* **2016**, *21*, 218-222.

[6] Bourg, S., Geist, A., Narbutt, J., The EURATOM FP7 project on actinide separation from spent nuclear fuels*, Nukleonika* **2015**, *60*, 809-814.

[7] www.geniors.eu.

[8] Bourg, S., Hill, C., Caravaca, C., Rhodes, C., Ekberg, C., Taylor, R., Geist, A., Modolo, G., Cassayre, L., Malmbeck, R., Harrison, M., de Angelis, G., Espatero, A., Bouvet, S., Ouvrier, N., ACSEPT—Partitioning technologies and actinide science: Towards pilot facilities in Europe*, Nucl. Eng. Des.* **2011**, *241*, 3427-3435.

[9] Lewis, F. W., Hudson, M. J., Harwood, L. M., Development of Highly Selective Ligands for Separations of Actinides from Lanthanides in the Nuclear Fuel Cycle*, Synlett* **2011**, *18*, 2609-2632.

[10] Taylor, R., *Reprocessing and Recycling of Spent Nuclear Fuel*, First ed., Woodhead Publishing, Oxford, **2015**.

[11] Baron, P., Berthon, L., Charbonnel, M. C., Nicol, C., in *in GLOBAL'97 (International Conference on Future Nuclear Systems)*, Atomic Energy Society of Japan, Yokohama, Japan, **1997**.

[12] Sasaki, Y., Sugo, Y., Suzuki, S., Tachimori, S., The Novel Extractants, Diglycolamides, for the Extraction of Lanthanides and Actinides in HNO_3 – n-Dodecane System*, Solv. Extr. Ion Exch.* **2001**, *19*, 91-103.

[13] Whittaker, D., Geist, A., Modolo, G., Taylor, R., Sarsfield, M., Wilden, A., Applications of Diglycolamide Based Solvent Extraction Processes in Spent Nuclear Fuel Reprocessing, Part 1: TODGA*, Solv. Extr. Ion Exch.* **2018**, *36*, 223-256.

[14] Sugo, Y., Izumi, Y., Yoshida, Y., Nishijima, S., Sasaki, Y., Kimura, T., Sekine, T., Kudo, H., Influence of diluent on radiolysis of amides in organic solution*, Radiat. Phys. Chem.* **2007**, *76*, 794-800.

[15] Galán, H., Núñez, A., Espartero, A. G., Sedano, R., Durana, A., de Mendoza, J., Radiolytic Stability of TODGA: Characterization of Degraded Samples under Different Experimental Conditions*, Procedia Chem.* **2012**, *7*, 195-201.

[16] Galán, H., Zarzana, C. A., Wilden, A., Nunez, A., Schmidt, H., Egberink, R. J. M., Leoncini, A., Cobos, J., Verboom, W., Modolo, G., Groenewold, G. S., Mincher, B. J., Gamma-radiolytic stability of new methylated TODGA derivatives for minor actinide recycling*, Dalton Trans.* **2015**, *44*, 18049-18056.

[17] Zarzana, C. A., Groenewold, G. S., Mincher, B., Mezyk, S. P., Wilden, A., Schmidt, H., Modolo, G., Wishart, J. F., Cook, A. R., A Comparison of the γ-Radiolysis of TODGA and T(EH)DGA Using UHPLC-ESI-MS Analysis*, Solv. Extr. Ion Exch.* **2015**, *33*, 431-447.

[18] Hubscher-Bruder, V., Mogilireddy, V., Michel, S., Leoncini, A., Huskens, J., Verboom, W., Galán, H., Nunez, A., Cobos, J., Modolo, G., Wilden, A., Schmidt, H., Charbonnel, M. C., Guilbaud, P., Boubals, N., Behaviour of the extractant Me-TODGA upon gamma irradiation: quantification of degradation compounds and individual influences on complexation and extraction*, New J. Chem.* **2017**, *41*, 13700-13711.

[19] Wilden, A., Schreinemachers, C., Sypula, M., Modolo, G., Direct Selective Extraction of Actinides (III) from PUREX Raffinate using a Mixture of $CyMe_4BTBP$ and TODGA as 1-cycle SANEX Solvent*, Solv. Extr. Ion Exch.* **2011**, *29*, 190-212.

[20] Magnusson, D., Christiansen, B., Foreman, M. R. S., Geist, A., Glatz, J. P., Malmbeck, R., Modolo, G., Serrano-Purroy, D., Sorel, C., Demonstration of a SANEX Process in Centrifugal Contactors using the $CyMe_4$-BTBP Molecule on a Genuine Fuel Solution*, Solv. Extr. Ion Exch.* **2009**, *27*, 97-106.

[21] Lewis, F. W., Harwood, L. M., Hudson, M. J., Drew, M. G., Desreux, J. F., Vidick, G., Bouslimani, N., Modolo, G., Wilden, A., Sypula, M., Vu, T. H., Simonin, J. P., Highly efficient separation of actinides from lanthanides by a phenanthroline-derived bis-triazine ligand*, J. Am. Chem. Soc.* **2011**, *133*, 13093-13102.

[22] Lange, S., Wilden, A., Modolo, G., Sadowski, F., Gerdes, M., Bosbach, D., Direct Selective Extraction of Trivalent Americium from PUREX Raffinate Using a Combination of $CyMe_4BTPhen$ and TEDGA—A Feasibility Study*, Solv. Extr. Ion Exch.* **2017**, *35*, 161-173.

[23] Magnusson, D., Christiansen, B., Malmbeck, R., Glatz, J.-P., Investigation of the radiolytic stability of a $CyMe_4$-BTBP based SANEX solvent*, Radiochim. Acta* **2009**, *97*, 497-502.

[24] Schmidt, H., Wilden, A., Modolo, G., Švehla, J., Grüner, B., Ekberg, C., Gamma radiolytic stability of $CyMe_4BTBP$ and the effect of nitric acid*, Nukleonika* **2015**, *60*, 879-884.

[25] Schmidt, H., Wilden, A., Modolo, G., Bosbach, D., Santiago-Schübel, B., Hupert, M., Švehla, J., Grüner, B., Ekberg, C., Gamma Radiolysis of the Highly Selective Ligands $CyMe_4BTBP$ and

CyMe$_4$BTPhen: Qualitative and Quantitative Investigation of Radiolysis Products*, Procedia Chem.* **2016**, *21*, 32-37.

[26] Wilden, A., Modolo, G., Hupert, M., Santiago-Schübel, B., Löfström-Engdahl, E., Halleröd, J., Ekberg, C., Mincher, B. J., Mezyk, S. P., Gamma-Radiolytic Stability of Solvents Containing C5-BPP (2,6-Bis(5-(2,2-dimethylpropyl)-1H-pyrazol-3-yl)pyridine) for Actinide(III)/Lanthanide(III) Separation*, Solv. Extr. Ion Exch.* **2016**, *34*, 1-12.

[27] Kondé, J., Distler, P., John, J., Švehla, J., Grüner, B., Bělčická, Z., Radiation Influencing of the Extraction Properties of the CyMe$_4$-BTBP and CyMe$_4$-BTPhen Solvents with FS-13*, Procedia Chem.* **2016**, *21*, 174-181.

[28] Billard, I., Ouadi, A., Gaillard, C., Liquid-liquid extraction of actinides, lanthanides, and fission products by use of ionic liquids: from discovery to understanding*, Anal. Bioanal. Chem.* **2011**, *400*, 1555-1566.

[29] Kolarik, Z., Ionic Liquids: How Far Do they Extend the Potential of Solvent Extraction of f-Elements?*, Solv. Extr. Ion Exch.* **2013**, *31*, 24-60.

[30] Vasudeva Rao, P. R., Venkatesan, K. A., Rout, A., Srinivasan, T. G., Nagarajan, K., Potential Applications of Room Temperature Ionic Liquids for Fission Products and Actinide Separation*, Sep. Sci. Technol.* **2012**, *47*, 204-222.

[31] Sun, X., Luo, H., Dai, S., Ionic Liquids-Based Extraction: A Promising Strategy for the Advanced Nuclear Fuel Cycle*, Chem. Rev.* **2012**, *112*, 2100-2128.

[32] Bose, R. S. C., Kumaresan, R., Venkatesan, K. A., Gardas, R. L., Antony, M. P., Vasudeva Rao, P. R., Insights Into the Extraction of Am(III) by Aliquat-336 Based Ionic Liquids*, Sep. Sci. Technol.* **2014**, *49*, 2338-2345.

[33] Zsabka, P., Van Hecke, K., Adriaensen, L., Wilden, A., Modolo, G., Verwerft, M., Binnemans, K., Cardinaels, T., Solvent Extraction of Am(III), Cm(III), and Ln(III) Ions from Simulated Highly Active Raffinate Solutions by TODGA Diluted in Aliquat-336 Nitrate Ionic Liquid*, Solv. Extr. Ion Exch.* **2018**, *36*, 519-541.

[34] Zsabka, P., Van Hecke, K., Wilden, A., Modolo, G., Verwerft, M., Binnemans, K., Cardinaels, T., Selective extraction of americium from curium and the lanthanides by the lipophilic ligand CyMe$_4$BTPhen dissolved in Aliquat-336 nitrate ionic liquid*, Solv. Extr. Ion Exch.* **2019**, *Accepted for publication*.

[35] Venkateswara Rao, C., Rout, A., Venkatesan, K. A., Probing the absence of third phase formation during the extraction of trivalent metal ions in an ionic liquid medium*, New J. Chem.* **2019**, *43*, 5099-5108.

[36] Mincher, B. J.,*Radiation chemistry in the reprocessing and recycling of spent nuclear fuels,* in *Reprocessing and Recycling of Spent Nuclear Fuel* (Ed.: R. Taylor), Woodhead Publishing, Oxford, **2015**, pp. 191-211.

[37] Mincher Bruce, J., Mezyk Stephen, P., in *Radiochim. Acta, Vol. 97*, **2009**, pp. 519-534.

[38] Spinks, J. W. T., Woods, R. J., *An introduction to radiation chemistry*, John Wiley & Sons, Inc., New York, **1990**.

[39] Garaix, G., Venault, L., Costagliola, A., Maurin, J., Guigue, M., Omnee, R., Blain, G., Vandenborre, J., Fattahi, M., Vigier, N., Moisy, P., Alpha radiolysis of nitric acid and sodium nitrate with $^4He^{2+}$ beam of 13.5 MeV energy*, Radiation Physics and Chemistry* **2015**, *106*, 394-403.

[40] Mincher, B. J., Wishart, J. F., The Radiation Chemistry of Ionic Liquids: A Review*, Solv. Extr. Ion Exch.* **2014**, *32*, 563-583.

[41] Shkrob, I. A., Chemerisov, S. D., Wishart, J. F., The initial stages of radiation damage in ionic liquids and ionic liquid-based extraction systems*, J. Phys. Chem. B* **2007**, *111*, 11786-11793.

[42] Le Rouzo, G., Lamouroux, C., Dauvois, V., Dannoux, A., Legand, S., Durand, D., Moisy, P., Moutiers, G., Anion effect on radiochemical stability of room-temperature ionic liquids under gamma irradiation*, Dalton Trans.* **2009**, *31*, 6175-6184.

[43] Bossé, E., Berthon, L., Zorz, N., Monget, J., Berthon, C., Bisel, I., Legand, S., Moisy, P., Stability of [MeBu$_3$N][Tf$_2$N] under gamma irradiation*, Dalton Trans.* **2008**, 924-931.

[44] Dhiman, S. B., Goff, G. S., Runde, W., LaVerne, J. A., Gamma and heavy ion radiolysis of ionic liquids: A comparative study, *J. Nucl. Mat.* **2014**, *453*, 182-187.

[45] Jagadeeswara Rao, C., Venkatesan, K. A., Tata, B. V. R., Nagarajan, K., Srinivasan, T. G., Vasudeva Rao, P. R., Radiation stability of some room temperature ionic liquids, *Radiat. Phys. Chem.* **2011**, *80*, 643-649.

[46] Komasawa, I., Miyamura, M., Synergistic extraction of rare-earth elements by tri-n-octylmethylammonium nitrate and β-diketone, *J. Chem. Eng. Jpn.* **1991**, *24*, 306-311.

[47] Alok, R., Satendra, K., Athmaram, V. K., Siuli., M., Pailo, A. M., Complexation of Eu(III) in a Completely Incinerable Ionic Liquid System: A Luminescence Spectroscopy Approach, *ChemistrySelect* **2018**, *3*, 3029-3035.

[48] Rout, A., Venkatesan, K. A., Antony, M. P., Vasudeva Rao, P. R., Liquid–Liquid extraction of americium(III) using a completely incenerable ionic liquid system, *Sep. Purif. Technol.* **2016**, *158*, 137-143.

[49] Kessler, C., Burns, D., Mihailescu, L. C., Chiriotti, S., Key comparison BIPMRI(I)-K1 of the air-kerma standards of the SCK•CEN, Belgium and the BIPM in ^{60}Co gamma irradiation, *Metrologia* **2017**, *54*, 1-11.

[50] Galán, H., Zarzana, C. A., Wilden, A., Nunez, A., Schmidt, H., Egberink, R. J., Leoncini, A., Cobos, J., Verboom, W., Modolo, G., Groenewold, G. S., Mincher, B. J., Gamma-radiolytic stability of new methylated TODGA derivatives for minor actinide recycling, *Dalton Trans.* **2015**, *44*, 18049-18056.

[51] Mezyk, S. P., Cullen, T. D., Rickman, K. A., Mincher, B. J., The Reactivity of the Nitrate Radical ($^{\bullet}NO_3$) in Aqueous and Organic Solutions, *Int. J. Chem. Kin.* **2017**, *49*, 635-642.

[52] Poskrebyshev, G. A., Neta, P., Huie, R. E., Equilibrium constant of the reaction $\cdot OH + HNO_3 \leftrightarrows H_2O + NO_3^{\cdot}$ in aqueous solution, *J. Geophys. Res.* **2001**, *106*, 4995-5004.

[53] Ng, N. L., Brown, S. S., Archibald, A. T., Atlas, E., Cohen, R. C., Crowley, J. N., Day, D. A., Donahue, N. M., Fry, J. L., Fuchs, H., Griffin, R. J., Guzman, M. I., Herrmann, H., Hodzic, A., Iinuma, Y., Jimenez, J. L., Kiendler-Scharr, A., Lee, B. H., Luecken, D. J., Mao, J., McLaren, R., Mutzel, A., Osthoff, H. D., Ouyang, B., Picquet-Varrault, B., Platt, U., Pye, H. O. T., Rudich, Y., Schwantes, R. H., Shiraiwa, M., Stutz, J., Thornton, J. A., Tilgner, A., Williams, B. J., Zaveri, R. A., Nitrate radicals and biogenic volatile organic compounds: oxidation, mechanisms, and organic aerosol, *Atmos. Chem. Phys.* **2017**, *17*, 2103-2162.

[54] Buxton, G. V., Greenstock, C. L., Helman, W. P., Ross, A. B., Critical review of rate constants for reactions of hydrated electrons, hydrogen atoms and hydroxyl radicals ($^{\bullet}OH/^{\bullet}O^{-}$) in aqueous solution, *J. Phys. Chem. Ref. Data* **1988**, *17*, 513-886.

[55] Allen, D., Baston, G., Bradley, A. E., Gorman, T., Haile, A., Hamblett, I., Hatter, J. E., Healey, M. J. F., Hodgson, B., Lewin, R., Lovell, K. V., Newton, B., Pitner, W. R., Rooney, D. W., Sanders, D., Seddon, K. R., Sims, H. E., Thied, R. C., An investigation of the radiochemical stability of ionic liquids, *Green Chem.* **2002**, *4*, 152-158.

[56] Elliot, A. J., Simsons, A. S., Reactions of NO_2 and nitrite ion with organic radicals, *Can. J. Chem.* **1984**, *62*, 1831-1834.

[57] Ikeda, H., Suzuki, A., Radiolysis of n-dodecane and Its Physical Property Change Based on the Dose in One Pass through a Reference HA Column, *J. Nucl. Sci. Technol.* **1998**, *35*, 697-704.

[58] Mincher, B. J., Curry, R. D., Considerations for choice of a kinetic fig. of merit in process radiation chemistry for waste treatment, *Appl. Radiat. Isot.* **2000**, *52*, 189-193.

[59] Roscioli-Johnson, K. M., Zarzana, C. A., Groenewold, G. S., Mincher, B. J., Wilden, A., Schmidt, H., Modolo, G., Santiago-Schübel, B., A Study of the γ-Radiolysis of N,N-Didodecyl-N′,N′-Dioctyldiglycolamide Using UHPLC-ESI-MS Analysis, *Solv. Extr. Ion Exch.* **2016**, *34*, 439-453.

[60] Nave, S., Modolo, G., Madic, C., Testard, F., Aggregation Properties of N,N,N′,N′-Tetraoctyl-3-oxapentanediamide (TODGA) in n-Dodecane, *Solv. Extr. Ion Exch.* **2004**, *22*, 527-551.

[61] Atkins, P. W., *Physical chemistry*, 6th ed., Oxford : Oxford university press, **2000**.